The Pennsylvania State University

The Graduate School

College of Medicine

EFFECTS OF AGING, IMMOBILIZATION AND HIGH FAT DIET ON ALTERNATIVE SPLICING OF FAST TROPONIN T IN RAT GASTROCNEMIUS MUSCLE

A Thesis in

Biomedical Sciences

by

Suhana Ravi

Submitted in Partial Fulfillment

of the Requirements

for the Degree of

Master of Science

August 2015

The thesis of Suhana Ravi was reviewed and approved* by the following:

Scot R. Kimball
Professor of Cellular and Molecular Physiology
Thesis Adviser

Leonard S. Jefferson, Jr.
Evan Pugh Professor of Cellular and Molecular Physiology

Lisa M. Shantz
Associate Professor of Cellular and Molecular Physiology

Ralph L. Keil
Associate Professor of Biochemistry and Molecular Biology
Chair, Biomedical Sciences Graduate Program

* Signatures are on file in the Graduate school.

ABSTRACT

Fast Troponin T (Tnnt3) is an important component of the skeletal muscle contractile machinery. Alternative splicing of the *Tnnt3* pre-mRNA results in generation of several splice forms that can be classified into two major categories based on whether they include mutually exclusive exon 16 (referred to as *Tnnt3α* splice forms) or 17 (referred to as *Tnnt3β* splice forms). Previous studies have shown that an increase in experienced body weight (i.e. actual body mass plus addition of external load) leads to a proportionate increase in relative abundance of *Tnnt3α* splice forms and a decrease in relative abundance of *Tnnt3β* splice forms. The *Tnnt3α* and *Tnnt3β* splice forms have been associated with increased and decreased calcium sensitivity respectively. The changes in alternative splicing pattern that occur in response to an increase in experienced body weight causes an overall enhancement in calcium sensitivity and force production resulting in improved skeletal muscle function in order to support the increased body weight. Hence, *Tnnt3* splice forms have distinctive effects on force production during muscle contraction, thereby regulating muscle function.

The work described in this thesis is focused on determining the variation in *Tnnt3* alternative splicing patterns in rat gastrocnemius muscles in response to different physiological conditions of impaired muscle function such as aging, skeletal muscle disuse and high fat diet-induced obesity. The studies presented here show that the relative abundance of several *Tnnt3* splice forms varied significantly among 2, 9 and 18-month old rats and the pattern of alternative splicing correlated with changes in body weight rather than muscle mass. Skeletal muscle disuse due to hindlimb immobilization for 7 days resulted in dramatic alterations in relative abundance of *Tnnt3* splice forms such that

the alternative splicing pattern was similar to that observed in lighter animals, i.e. decreased relative abundance of *Tnnt3α* splice forms and increased relative abundance of *Tnnt3β* splice forms. Remobilization for 7 days after hindlimb immobilization restored the relative abundance of most *Tnnt3* splice forms toward that observed in the non-immobilized limb, even though muscle mass had not yet begun to recover. High fat diet consumption for 2 and 8 weeks also resulted in body weight-inappropriate patterns of *Tnnt3* alternative splicing. There was an overall decrease in relative abundance of *Tnnt3α* splice forms and an increase in relative abundance of *Tnnt3β* splice forms.

In conclusion, these studies demonstrate that alternative splicing of *Tnnt3* pre-mRNA is disrupted during early stages of skeletal muscle disuse and high fat diet-induced obesity. The alternative splicing pattern is shifted such that there is an overall decrease in calcium sensitivity and force production. This could be a potential mechanism for disuse and obesity-related decline in skeletal muscle function.

TABLE OF CONTENTS

LIST OF FIGURES

LIST OF TABLES

ACKNOWLEDGEMENTS

"All that we behold is full of blessings." – William Wordsworth

The three years that I have spent in Penn State Hershey, although incredibly tumultuous, have been the most gratifying years of my life. My wonderful mentors and friends in Hershey have stood by me through every single phase of my career and I consider myself truly blessed for having met them. First and foremost, I thank God for guiding me on this remarkable journey and giving me the strength to bravely handle every situation with confidence and determination.

I am highly indebted to my thesis adviser, Dr. Scot Kimball, for his invaluable guidance and expertise. Thank you for always having faith in my capabilities and motivating me to strive towards diligence and perfection. My heartfelt thanks to Dr. Jim Jefferson for helping me to take a holistic approach for my thesis research. Your helpful suggestions have been instrumental in data interpretation and preparation of manuscripts. Dr. Ralph Keil has been a tremendous source of encouragement and inspiration. Thank you for helping me realize my own strengths and grow into a confident, brave and independent person. I would like to thank my committee members, Dr. Lisa Shantz and Dr. Jim Marden, for their support. I am extremely grateful to Dr. Arthur Berg for guidance in performing statistical analyses for my project. I acknowledge the National Institutes of Health (NIH grant DK094141 - S.R.K. and NIH grant DK13499 – L.S.J.) and Abbott Nutrition for providing financial support for my thesis research.

A special thank you to Dr. Brad Gordon for helping me carry out rat studies, teaching me lab techniques and patiently answering my innumerable questions. Your pranks, jokes and optimism have motivated me to face each new day with a smile. I owe immense gratitude to Dr. Ruud Schilder for helpful inputs in experimental techniques and data analyses. I would like to thank Sharron Rannels, Holly Lacko, Lydia Kutzler, Dr. Michael Dennis, Dr. Andrew Kelleher, Tony Martin, Adam Black and Chen Yang for always being there to help me with lab work, discuss ideas and talk about day-to-day issues. Thank you for making Hershey feel like a second home to me. Many thanks to all my loving friends, especially Vasudha, Prashanth, Sreeram, Amriti and Smita.

All that I am, I owe to my parents. Thank you for giving me the courage and strength to pursue my dreams. A big hug to my adorable brother for being patient with me when I was busy with lab work and showering me with so much attention. Without the three of you by my side, writing this thesis would not have been such an enjoyable experience. Thanks to my wonderful grandparents for always believing in me. I dedicate this thesis and all my accomplishments to my loving family.

Chapter 1.

INTRODUCTION

Precursor mRNA splicing

In mammals, gene expression involves a number of steps starting with the transcription of a gene into precursor mRNA (pre-mRNA), that is usually processed into mature mRNA that is exported from the nucleus for translation to protein by cytoplasmic ribosomes. Many studies have focused on the regulation of the first and last steps in gene expression, i.e. DNA transcription and mRNA translation. Pre-mRNA splicing is also a well-regulated process and is a critical intermediate step in gene expression that results in the conversion of pre-mRNA into mature mRNA that can be translated into protein (1).

In mammalian pre-mRNAs, introns are removed by two trans-esterification reactions catalyzed by the spliceosome and associated auxiliary proteins that result in removal of an intron and the joining of the two exons that border the intron leading to formation of mature mRNA (1) (Figure 1.1). The core of the spliceosome is comprised of a complex of five small nuclear ribonucleoprotein particles (snRNPs) that are recruited to the pre-mRNA in a sequence-dependent manner. The splicing process is under robust regulation to ensure temporal and cell- and tissue-specific expression of splice variants. Part of this regulation is due to the utilization of distinct snRNPs and auxiliary proteins for different types of splicing events. At least 45 snRNPs have been identified as components of the spliceosome and more than 170 auxiliary proteins are known to

regulate the process. Splicing is dynamic and remodeling of RNA-protein and protein-protein interactions mediates progression of the machinery along the pre-mRNA.

The pre-mRNA includes 3'- and 5'-splice sites located at exon-intron junctions and these sites recruit specific proteins of the spliceosome by base pairing with the snRNPs (1). Splice site recognition is further mediated by cis- and trans-regulatory elements (Figure 1.1). The cis-regulatory elements are present within the pre-mRNA in regions proximal to the splice site and include intronic or exonic sequences that recruit auxiliary proteins (i.e. trans-regulatory elements or factors) that regulate spliceosomal assembly. Trans factors are broadly classified as splicing enhancers, e.g., serine/arginine-rich proteins (SR proteins), that facilitate splice site recognition by the spliceosome, or splicing repressors, e.g., heterogeneous nuclear ribonucleoproteins (hnRNPs) that inhibit splice site recognition (2). However, some splicing factors like hnRNP L and hnRNP H can act either as enhancers or repressors depending on the type of cis element to which they are bound or the location of the cis element in the pre-mRNA. Importantly, the binding of trans factors to the cis elements can be modulated in response to environmental cues (e.g., hormones and nutrients) through phosphorylation of trans factors such as the SR proteins (2, 3). The efficiency of the splicing process depends on the activity, i.e. phosphorylation status, and abundance of trans factors, i.e., competitive and mutually exclusive binding to the cis elements.

There are two types of splicing processes (Figure 1.1) (1-3). Constitutive splicing mediates the removal of introns and inclusion of all exons in the mature mRNA (e.g., glucose-6-phosphate dehydrogenase – G6PD (4)). Defective regulation of this process results in unspliced transcripts that cannot be translated into proteins and are degraded by

RNA-mediated decay. Alternative splicing is the process whereby alternative exons and/or introns are selectively in- or excluded, generating multiple mature mRNAs called splice forms or splice variants (e.g., Troponin T (5)). Different processes such as intron retention, exon skipping, mutually exclusive exon inclusion/exclusion, and alternative 5'- or 3'-splice site usage are involved. Recent estimates suggest that 95% or more of human pre-mRNAs are subject to alternative splicing, while in other organisms this number is much lower (e.g., ~40% in *Drosophila*) (6). The number of mature mRNAs that can be generated from a single pre-mRNA varies widely, with some pre-mRNAs predicted to generate as many as several thousand mature mRNAs. However, the abundance of some alternatively spliced mature mRNAs is low (i.e., <1% of the total) and the number of functionally distinct proteins produced by alternative pre-mRNA splicing is undoubtedly much smaller than the number of possible alternative splicing events predicted solely by splice site identification. In most cases, the splice forms have distinctive physiological effects due to changes in sub cellular localization, protein-protein interactions or flux through metabolic pathways (1, 2). Alternative splicing is fundamental for different stages of embryonic development and abnormal regulation has been linked to several diseases such as diabetes, obesity and cancer. While basic mechanisms of pre-mRNA alternative splicing of introns and exons are reasonably well characterized, how these mechanisms are regulated remains poorly understood.

Troponin T – chief regulator of skeletal muscle function

Skeletal muscle accounts for almost 50% of the total body mass in humans and skeletal muscle contraction is a well-regulated process that controls movement (7). The contractile unit of skeletal muscle is the sarcomere, which is composed of thick filaments comprised of myosin and thin filaments consisting of actin, tropomyosin and troponin (8-10). When the globular head of myosin is not bound to ATP, it can tightly bind to actin to form a cross-bridge. This interaction between the thick and thin filaments is fundamental for force production during muscle contraction. When the myosin head is bound to ATP, it dissociates from actin and can hydrolyze the bound ATP molecule due to its ATPase activity. The energy thus produced causes conformational changes in myosin and the myosin head binds to another position on actin located further along the thin filament to form a new cross-bridge. The myosin head converts the chemical energy from ATP hydrolysis into mechanical energy. Hence, repeated cycles of actin-myosin interaction, detachment and ATP hydrolysis result in muscle contraction by generating the force required for displacement of thin filaments across the thick filaments leading to shortening of the sarcomere. Muscle contraction can be initiated only in the presence of high concentrations of cytoplasmic calcium (Ca^{2+}). Under conditions of low concentrations of cytoplasmic Ca^{2+}, muscle relaxation occurs and the sarcomere extends to its resting length.

Cross-bridge formation and muscle contraction is regulated by the actin binding proteins – tropomyosin and troponin - that are also part of the thin filament (8-10). Troponin is a heterotrimeric complex consisting of troponin C (TnC) that can bind to Ca^{2+}, troponin T (TnT) that binds to tropomyosin and troponin I (TnI) that binds to actin

to inhibit actin-myosin interaction. In the absence of Ca^{2+}, tropomyosin (Tm) associates with actin and blocks the myosin binding sites, thus preventing actin-myosin interaction and thereby inhibiting muscle contraction. A single Tm molecule extends across seven actin molecules in the thin filament and the head-to-tail overlapping of adjacent Tm molecules allows the intertwining of tropomyosin with actin. In addition to physically preventing the binding of actin to myosin in the absence of calcium, the troponin-Tm complex has been shown to inhibit myosin ATPase activity by blocking a kinetic step in ATP hydrolysis. Upon stimulation of muscle fibers by nerve impulses, Ca^{2+} is released from the sarcoplasmic reticulum into the cytoplasm and binds to TnC. This causes conformational changes in the troponins and tropomyosin slides over actin to expose the myosin binding sites. This is followed by multiple cycles of cross-bridge formation, dissociation and ATP hydrolysis, leading to muscle contraction.

TnT is considered as the "structural glue" that holds the proteins of the thin filament together (11). Ferrante et al. showed that TnT is crucial for normal assembly of the sarcomere components (12). Thin filaments did not form in the TnT-depleted skeletal muscles of zebrafish due to abnormal aggregation of actin, dysregulation of actin-myosin interaction and disrupted association of actin with tropomyosin.

Although TnT does not directly bind to Ca^{2+}, it is necessary for Ca^{2+} sensitivity and complete activation/inhibition of myosin ATPase activity during muscle contraction/relaxation (11, 13, 14). This function of TnT can be attributed to its interactions with Tm, TnI and TnC. The structure of TnT is a single polypeptide chain (molecular weight 31-36 kDa) that contains an N-terminal region, a middle region and a C-terminal region (Figure 1.2). The TnT N-terminal region is involved in the activation

of myosin ATPase after actin-myosin interactions are established in the presence of Ca^{2+}. The TnT middle region interacts with the C-terminal region of Tm and extends to the head-to-tail overlap region of two adjacent Tm molecules. In the presence of Ca^{2+}, these TnT-Tm interactions coordinate the sliding of Tm across actin to allow actin-myosin binding. The TnT C-terminal region has another binding site for Tm and can also interact with TnI, TnC and actin. In the absence of Ca^{2+}, the TnT C-terminal region binds to Tm and inhibits the effect of the TnT N-terminal region on the activation of myosin ATPase activity. TnT is essential for the rapid, Ca^{2+}-dependent structural transitions in the troponin complex. In the presence of Ca^{2+}, the affinity of TnC for TnI increases and the TnI-actin interaction is weakened so that actin-myosin binding can occur. In addition to Ca^{2+} sensitivity, TnT is necessary for cooperativity of the conformational changes in the thin filament and actin-myosin interaction during muscle contraction.

Alternative splicing of troponin T pre-mRNA

In vertebrates, skeletal muscle fibers can be classified into two types – slow (type I) and fast (type II) fibers – that express two different genes encoding TnT, namely slow *Tnnt1* and fast *Tnnt3* (5). The invertebrate *TnT* gene is homologous to fast skeletal *Tnnt3* in vertebrates. Alternative splicing of pre-mRNAs of *Tnnt3* and *TnT* is evolutionarily conserved and gives rise to splice forms that can be translated into proteins with different conformational and functional characteristics (5, 15-21). In skeletal muscle of mammals such as rabbit (5, 19, 22), rat (5, 18, 19) and human (20), a large number of splice forms are expressed, albeit some at low levels. There are many difficulties in studying the structure and function of the full repertoire of TNNT3 splice forms, such as the absence

of high resolution three-dimensional complete structures for TNNT3 and the lack of evidence for expression of all *Tnnt3* splice forms at the protein level.

Medford et al. classified the *Tnnt3* splice forms based on the presence of two mutually exclusive exons 16 and 17 at the 3'end of the *Tnnt3* pre-mRNA (16). *Tnnt3α* splice forms contain exon 16 and *Tnnt3β* splice forms contain exon 17. *α* and *β* splice forms differ in the sequence encoding the C-terminal region of TNNT3 that can interact with Tm, TnI, TnC and actin, as described above. Hence, the proteins encoded by *α* and *β* splice forms (TNNT3α and TNNT3β respectively) have distinctive effects on the Ca^{2+} sensitivity of the thin filament during muscle contraction (23, 24). TNNT3α has higher affinity for Tm and interacts more strongly with TnC, when compared to TNNT3β (23, 25, 26). In the presence of TNNT3α, the affinity of TnC for Ca^{2+} is three-fold higher than in the presence of TNNT3β. Gallon et al. showed that reconstitution of rat psoas muscle fibers with TNNT3α made the fibers more sensitive to Ca^{2+} and reconstitution with TNNT3β made the fibers less Ca^{2+} sensitive (24). Exon 17 of fast *Tnnt3* is homologous to the counterpart exon of slow *Tnnt1* but exon 16 of fast *Tnnt3* shows less similarity to the counterpart exon of slow *Tnnt1*, indicating that the *Tnnt3α* splice forms are an evolutionary adaptation to improve the functional performance of fast skeletal muscles (27). Exon 16 of *Tnnt3* encodes a more hydrophobic TNNT3 C-terminal region when compared to exon 17 and so, the splice forms alter the overall stability of the troponin complex (25).

Exons 4, 5, 6, 7 and 8 in the 5'end of the *Tnnt3* pre-mRNA also undergo extensive alternative splicing (5, 27). This portion of the *Tnnt3* pre-mRNA encodes the N-terminal region of TnT. Although this region does not interact with any of the sarcomere

components, deletion or mutation of this region alters the affinity of TnT for Tm and modifies the overall conformation of TnT so that its interactions with TnC and TnI are altered. Briggs et al. showed that fast skeletal muscle fibers with increased abundance of *Tnnt3* splice forms that lack exon 4 have increased Ca^{2+} sensitivity (19). Such fibers also have shorter contraction time and higher velocity of muscle shortening (19, 22).

Regulation of troponin T pre-mRNA alternative splicing

An important function of the skeletal muscle is to provide support for total body weight in order to coordinate locomotion (7). The contractile function of the sarcomere can be altered in response to the mechanical load imposed by body weight. Marden et al. showed that the pattern of *TnT* alternative splicing is adjusted in insect flight muscles following changes in body weight (28). In the flight muscles of armyworm moths and fritillary butterflies, increase in body weight corresponds to a proportionate increase in abundance of larger *TnT* splice forms associated with increased calcium sensitivity, force production and power output, relative to all *TnT* splice forms. This change in abundance of *TnT* splice forms correlates with increased metabolic rate of flight muscles in moths and increased activity in butterflies. Similar to the effect of natural increase in body weight during insect growth phases, the addition of experimental loads for 5 days also results in increased relative abundance of larger *TnT* splice forms, indicating that the changes in *TnT* alternative splicing occur in response to changes in gravitational load on the flight muscles.

In mammals, the gastrocnemius and soleus are the most powerful muscles in the hindlimb and the gastrocnemius is primarily responsible for supporting the body weight during movement (29). The soleus is composed of mostly slow muscle fibers (30) that

produce lower forces when compared to fast fibers and do not express *Tnnt3* (5), whereas the gastrocnemius contains both slow and fast muscle fibers (30) and so *Tnnt3* is expressed at significant levels (5). Schilder et al. quantified the effects of natural and experimental increases in body weight on the alternative splicing patterns of fast skeletal *Tnnt3* (homologous to insect *TnT*) in rat gastrocnemius muscles (18). Increase in body weight (both natural and after addition of experimental load for 5 days) results in a proportionate increase in relative abundance of all *Tnnt3α* splice forms associated with increased Ca^{2+} sensitivity and a decrease in relative abundance of most of the *Tnnt3β* splice forms associated with decreased Ca^{2+} sensitivity. In addition, there is increased abundance of exon 4-lacking *Tnnt3* splice forms associated with increased Ca^{2+} sensitivity and decreased abundance of exon 4-containing *Tnnt3* splice forms. This change in *Tnnt3* alternative splicing correlates with increased energy expenditure during ambulatory activity.

Apart from body weight, different larval feeding regimens in insects also affect *TnT* alternative splicing patterns (28). There is increased abundance of larger *TnT* splice forms associated with improved force production and higher metabolic rate in flight muscles of larvae exposed to better nutritional status (i.e. freely fed larvae and larvae that experienced short periods of food restriction). Although these feeding regimens contribute to higher body weight when compared to regimens with longer periods of food restriction, the effect on *TnT* alternative splicing is independent of body weight. This indicates that nutrition can have direct effects on muscle function by modulating *TnT* alternative splicing patterns.

There is a paucity of information about molecular mechanisms for regulation of *Tnnt3* alternative splicing. The Akt (protein kinase B) signaling pathway is important for regulation of various splicing events such as protein kinase C alternative splicing in insulin-stimulated skeletal muscle cells (31). Schilder et al. showed that inhibition of Akt kinase activity disrupts mechanical loading-induced *Tnnt3* alternative splicing in cultured mouse skeletal muscle cells (32). A few studies have linked muscleblind-like 1 (MBNL1) to the regulation of *Tnnt3* alternative splicing (33-35). MBNL1 is a tissue-specific splicing factor that is specifically expressed in cardiac and skeletal muscle and can activate or repress splicing events depending on the location of its binding site in intronic regions of pre-mRNAs. It regulates alternative splicing of sarcomere components like actinin, titin and troponins during different stages of muscle development. In MBNL1 knockout mice, there is aberrant *Tnnt3* alternative splicing in skeletal muscles wherein a fetal exon is retained between exon 8 and 9 at the 5' end of *Tnnt3* pre-mRNA (33). The phenotype of these mice is similar to myotonic dystrophy in humans, with development of muscle weakness in neonates due to delayed muscle relaxation, possibly due to the defective *Tnnt3* alternative splicing.

Physiological conditions affecting skeletal muscle function

Skeletal muscles are highly adaptable to physiological demands and muscle contractile function can be rapidly altered to produce appropriate force to perform a wide range of activities (7, 36-38). This plasticity of skeletal muscles is achieved by alterations in contractile properties of sarcomere components, primarily myosin, troponin and tropomyosin (39). For example, mechanical loading due to increase in body weight alters the relative abundance of *Tnnt3* splice forms such that Ca^{2+} sensitivity is increased and so

more actin-myosin cross-bridges can be activated to generate more force in order to support the increased body weight (18, 28). The opposite effect i.e. decreased skeletal muscle force production is seen in mechanical unloading due to skeletal muscle disuse and physical inactivity and disease states such as cancer, sarcopenia due to aging, obesity and muscular dystrophy (7, 36-38). Abnormal *Tnnt3* alternative splicing could be a potential mechanism for the impaired muscle function in these conditions. Therefore, this thesis is aimed at determining the variation in *Tnnt3* alternative splicing patterns caused by three physiological conditions that lead to decline in skeletal muscle function – aging, disuse and high fat diet-induced obesity. Although these conditions have different causes and pathogenesis, several shared mechanisms for decreased muscle function, have been identified (7, 36-38).

Aging

Impaired skeletal muscle function due to aging is an important cause for increased fall risk, severely limited mobility and increased mortality in the elderly (40-44). Age-related sarcopenia is the progressive loss of muscle mass (also called skeletal muscle atrophy), particularly in the lower limbs (45). This is the primary mechanism for decline in skeletal muscle function and several studies have elucidated the signaling pathways involved such as mTORC1-mediated decrease in protein synthesis (46) and increase in protein degradation regulated by ubiquitin ligases like atrogin-1 (37). Interestingly, aging-related decline in muscle function is disproportionally greater than the predicted change based on loss of muscle mass, indicating that factors other than atrophy are also important in the regulation of muscle function (47-49). Aging also causes changes in muscle fiber composition, i.e. switching of fast to slow muscle fibers resulting in

decreased force production (45). The alterations in sarcomere components such as *Tnnt3* that result in these changes are not completely understood.

A recent study by Coble et al. showed that *Tnnt3* alternative splicing patterns are different among skeletal muscles of male subjects of two age groups - older (68 ± 2 years) and younger (27 ± 2 years) (50). In the older individuals, there is decreased abundance of *Tnnt3α* splice forms associated with increased Ca^{2+} sensitivity and increased abundance of *Tnnt3β* splice forms associated with decreased Ca^{2+} sensitivity, when compared to younger individuals. In support of previous studies on Ca^{2+} sensitivity of *Tnnt3* splice forms, the abundance of *Tnnt3α* splice forms has a positive linear correlation with muscle function, as determined by bilateral leg extension tests in both young and old subjects. However, the abundance of *Tnnt3β* splice forms has a negative linear correlation with muscle function. Therefore, the *Tnnt3* alternative splicing pattern in older individuals corresponds to lower Ca^{2+} sensitivity and impaired muscle function. In addition, there are no significant differences in lean mass amongst the younger and older individuals and so, changes in *Tnnt3* alternative splicing occur before the onset of atrophy during the early stages of muscle function decline due to aging.

Several studies have shown that Akt activity is downregulated in skeletal muscles in response to aging in humans and in rodent models (51). Maletesta et al. showed that MBNL1 is abnormally sequestered within the nucleus in skeletal muscles of aged rats and so, its activity as a splice factor is compromised (52). These aging-related disruptions in Akt and MBNL1 activities could be responsible for impaired *Tnnt3* alternative splicing.

Skeletal muscle disuse

Physical inactivity resulting in skeletal muscle disuse due to chronic bed rest (53), spinal cord injury (54) and limb immobilization (55) are some of the leading causes for muscle weakness in humans and have been linked to increased health care costs and risk for mortality in humans. Similar to aging, disuse also leads to loss of muscle mass and decreased force production (55-58). The molecular changes within the sarcomere that cause decline in muscle function have not been completely elucidated. Disuse results in mechanical unloading of skeletal muscles and would be predicted to modify *Tnnt3* alternative splicing patterns. Hindlimb suspension models for skeletal muscle disuse in rats show changes in abundance of TNNT3 splice forms in the soleus (59, 60). Akt activity is also decreased in soleus (61) and this could be a possible mechanism for abnormal *Tnnt3* alternative splicing. Changes in *Tnnt3* alternative splicing patterns and Akt signaling in response to disuse in muscles containing fast fibers such as gastrocnemius have not been studied.

An effective method to enable recovery of skeletal muscle atrophy following immobilization is to apply mechanical load on the disused muscle by remobilization (55). This leads to restoration of muscle mass and recovery of Akt signaling (61). Changes in *Tnnt3* alternative splicing in response to remobilization are not known. Amino acid supplementation also enhances recovery from atrophy by increasing muscle protein synthesis (61). These methods for recovery from disuse do not improve muscle force production and so there is an unmet need for therapeutic strategies targeting decline in muscle function. Moreover, the effect of disuse is exacerbated by aging and so skeletal muscles of older rats are more susceptible to mechanical unloading (62-64). Also,

recovery of aged muscles after disuse is challenging. Dietary protein supplementation during a 5-day leg immobilization period in healthy older male subjects (69 ± 1 years) does not lead to recovery of muscle mass and function (65). A detailed understanding of the alterations in sarcomere components after remobilization and the combined effects of aging and disuse is fundamental for designing therapeutic interventions to prevent and/or attenuate impaired skeletal muscle function.

Obesity and high fat diet

Obesity is a highly prevalent disease associated with co-morbidities such as diabetes and cardiovascular diseases and it increases the risk for different types of cancer like esophageal and pancreatic cancer (66-68). Apart from these conditions, obese individuals also suffer from severe restrictions to mobility due to insufficient functional capacity of skeletal muscle in supporting the excessive body weight, i.e. there is a significant decrease in relative skeletal muscle strength (muscle strength/body weight) (69). Several human studies show that obese individuals have decreased ability to perform daily activities like getting up from the chair, climbing the stairs etc. (70, 71). Obese women and children have decreased muscle function, as determined by hand grip and knee extension studies (72, 73).

The primary causes for excessive weight gain resulting in obesity are over-nutrition, i.e. excess energy intake, and physical inactivity, i.e. decreased energy expenditure (74, 75). Epidemiological studies have linked obesity susceptibility to the increased consumption of dietary saturated fatty acids that results in increased energy intake. There is a plethora of studies on rodent models for diet-induced obesity utilizing high fat diets (HFD), wherein a high percentage of energy (kcal) comes from saturated

fatty acids (76-81). These studies are mainly focused on mechanisms for insulin resistance and glucose uptake in the skeletal muscle and relatively few studies have considered obesity-related decline in muscle function (82-85). Shortreed et al. showed that HFD consumption by mice for 8 weeks affects muscle fibers in the gastrocnemius/plantaris complex to result in reduced force production and delayed recovery after fatigue (86). Similarly, Ciapaite et al. determined that after 5 weeks of HFD feeding, mouse soleus muscle shows decreased force production and extensor digitorum longus exhibits delayed relaxation (87). 16 weeks of high fat and high carbohydrate diet consumption causes decreased cross-sectional area of gastrocnemius, indicating that prolonged HFD leads to muscle atrophy and defective muscle function (77). The molecular mechanisms causing this decline in muscle function are not completely understood.

The body weight dependence of *Tnnt3* alternative splicing is impaired in gastrocnemius muscles of obese Zucker rats (18). The relative abundance of *Tnnt3β* splice forms in obese rats of higher body weight is similar to that of lean rats of lower body weight. This mismatch between body weight and *Tnnt3* alternative splicing patterns becomes worse at the later stages of obesity. In addition, there is decreased relative abundance of exon 4-lacking *Tnnt3* splice forms associated with increased Ca^{2+} sensitivity in obese rats. Hence, obesity results in altered patterns of *Tnnt3* alternative splicing such that the relative abundance of *Tnnt3* splice forms is not adequate for modulating muscle function to support body weight. These changes in *Tnnt3* alternative splicing patterns could be responsible for the decline in muscle function in obesity and the role of *Tnnt3* alternative splicing needs to be studied in HFD-induced obesity as well.

Several studies on rodent models for HFD-induced obesity have shown that excessive accumulation of lipids in skeletal muscles results in insulin resistance and decreased phosphorylation and activity of downstream effectors of insulin signaling such as Akt (77-81). This impairment of insulin-stimulated Akt activity could be responsible for aberrant *Tnnt3* alternative splicing leading to diminished skeletal muscle function associated with HFD-obesity.

Objectives of this thesis research

The research presented in this thesis is aimed at characterizing the variations in *Tnnt3* alternative splicing in rat gastrocnemius muscles in response to physiological conditions that result in decreased muscle function. In chapter 2, the effects of aging, skeletal muscle disuse due to hindlimb immobilization and remobilization after disuse will be discussed. In chapter 3, the effects of HFD feeding for different time periods will be described. The overall goal of this thesis is to determine whether there are changes in relative abundance of Tnnt3α and Tnnt3β splice forms associated with increased and decreased Ca^{2+} sensitivity, respectively, resulting in body weight inappropriate *Tnnt3* alternative splicing under these conditions.

Figure 1.1: Mechanisms for regulation of splicing by cis and trans factors

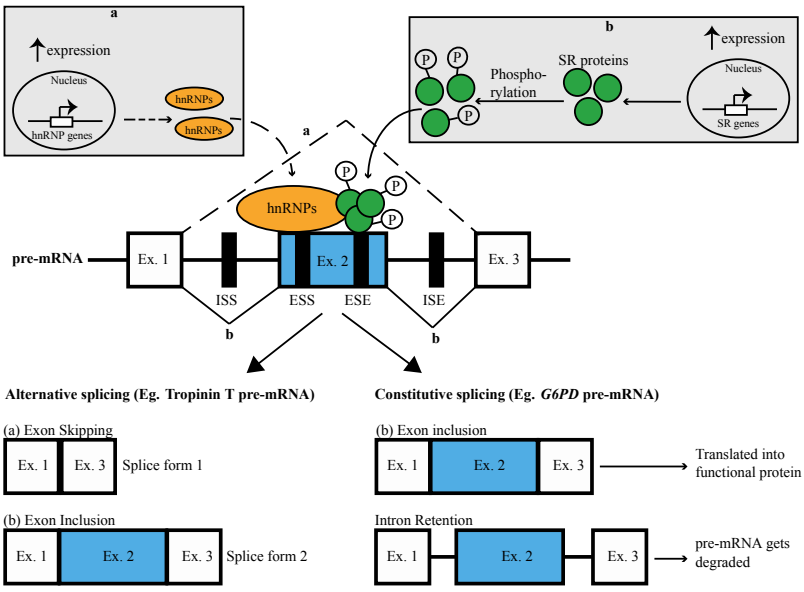

The pre-mRNA depicted in this cartoon consists of three exons, represented by white and grey boxes. The lines connecting the exons denote the introns that are removed during the splicing process. There are two types of splicing processes. Alternative splicing leads to different types of splice variants depending on which exons are included or excluded. In this example, exon 2 (Ex. 2) can be alternatively spliced and the outcome of splicing events is regulated by both cis elements (denoted by black boxes) and trans factors. (a) Due to increased expression, heterogeneous nuclear ribonucleoproteins (hnRNPs) can bind exonic splicing silencers (ESS) in Ex.2 to inhibit the assembly of splicing machinery at the intron-exon junction. As a result, Ex.2 is excluded from the mature mRNA and splice form 1 is formed. (b) Due to increased expression and phosphorylation, serine/arginine-rich proteins (SR proteins) bind to exonic splicing enhancers (ESE) within Ex.2 to promote its inclusion. The mature mRNA produced – splice form 2 – includes all the three exons. Constitutive splicing mediates the removal of introns and inclusion all exons in the mature mRNA that can be translated into a functional protein. Defective regulation of this process results in intron retention and the unspliced transcripts cannot be translated into proteins and are degraded by RNA-mediated decay pathways. Intronic splicing enhancers (ISE) and silencers (ISS) function similar to exonic elements.

Figure 1.2: Structure of troponin T and binding sites for tropomyosin, troponin C and troponin I

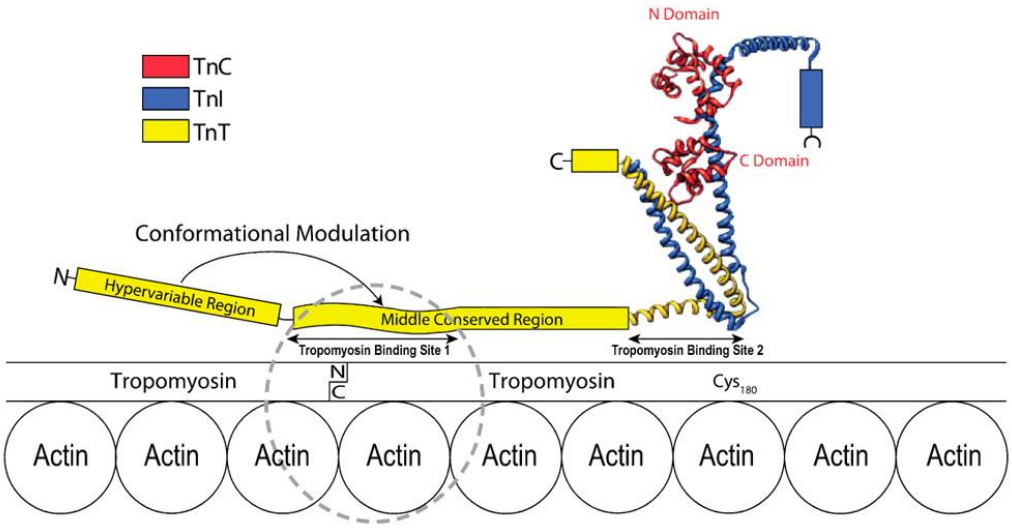

[adapted with permission from (27). Copyright (2015) American Chemical Society]

Troponin T (TnT) consists of three regions, the N-terminal region that does not bind to any of the sarcomere components, the middle region that binds to tropomyosin and the C-terminal region that binds to tropomyosin, troponin C (TnC) and troponin I (TnI). The N-terminal region is hypervariable and alternatively spliced exons 4 to 8 are located here. The C-terminal region contains the mutually exclusive exons 16 and 17.

Chapter 2.

MATERIALS AND METHODS

Quantification of *Tnnt3* splice forms

Frozen gastrocnemius muscles were pulverized under liquid nitrogen and total RNA was isolated using Trizol reagent as per the manufacturer's protocol (Invitrogen). cDNA was prepared using a High Capacity cDNA Reverse Transcription kit (Applied Biosystems), and PCR was carried out using GoTaq DNA polymerase (Promega) with a fluorescein-labeled forward primer and two reverse primers as previously described (Figure 2.1) (18). The fluorescein-labeled PCR amplicons were analyzed by capillary electrophoresis (3730XL DNA Analyzer, Applied Biosystems) and the fragment size of the PCR amplicons was determined using the 1200 LIZ internal size standard (Applied Biosystems). Peak Scanner software (Applied Biosystems) was used to sort the PCR amplicons based on predicted fragment size in order to annotate them as *Tnnt3* splice forms and determine fluorescent intensity (depicted as peak height) for the splice forms as a measure of their abundance (Figure 2.2).

The relative abundance of each *Tnnt3* splice form was calculated as the ratio of its detected peak height to the sum of all peak heights. This method was previously used to identify 12 *Tnnt3* splice forms (3 Tnnt3α splice forms and 9 Tnnt3β splice forms) in rat gastrocnemius muscle (Figure 2.1) (18). The total relative abundance of Tnnt3α and Tnnt3β splice forms was determined as the sum of relative abundances of individual Tnnt3α and Tnnt3β splice forms respectively.

Statistical Analyses

Statistical analyses were performed using Prism 6 (GraphPad Software, Inc.) and JMP Pro 10 (SAS Institute Inc.) as explained in detail in the following chapters. Principal component analysis was applied to reduce the 12-dimensional data sets for relative abundances of the 12 *Tnnt3* splice forms and the first two principal components were included in the analyses.

Figure 2.1: *Tnnt3* splice forms identified in rat gastrocnemius muscles

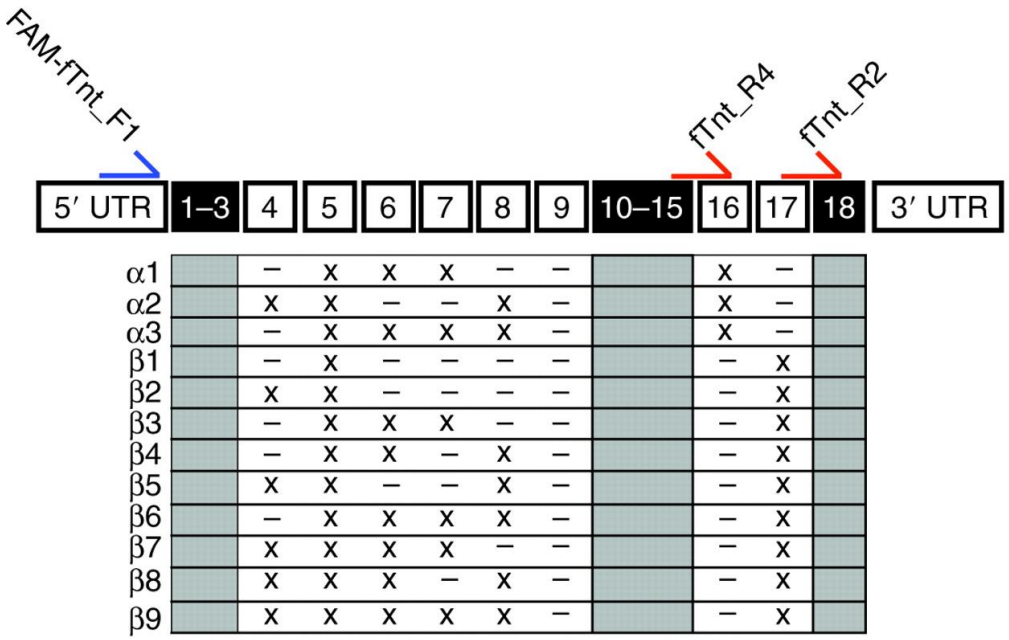

[adapted with permission from (18)]

The 12 *Tnnt3* splice forms in gastrocnemius muscles from male Sprague-Dawley rats are shown. The black boxes (exons 1-3, 10-15 and 18) represent constitutively spliced exons. The white boxes (exons 4 to 8 and exons 16 and 17) represent alternatively spliced exons. These splice forms can be amplified using the forward primer (F1) and two reverse primers (R4, R2).

Figure 2.2: Quantification of *Tnnt3* splice forms

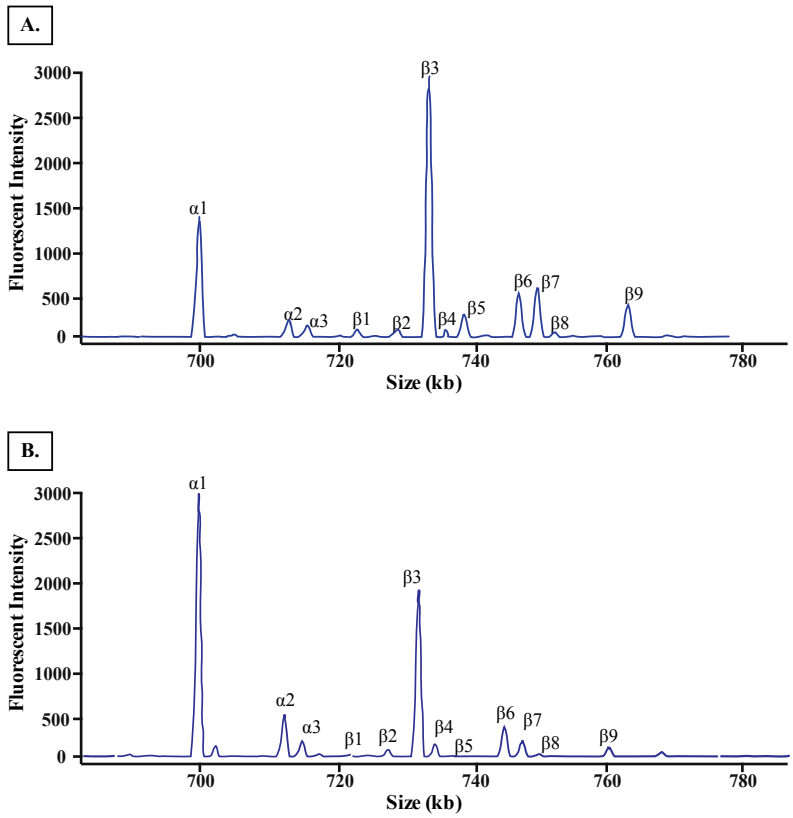

A representative trace of the fluorescently labeled PCR amplicons corresponding to the 12 *Tnnt3* splice forms in the gastrocnemius muscle of a 2-month old rat (A) and an 18-month old rat (B) as determined by capillary electrophoresis is shown. The fluorescent intensity for a particular splice form, i.e. the peak height, as determined using Peak Scanner software, is an indicator of the abundance of that splice form.

Chapter 3.

EFFECTS OF AGE, IMMOBILIZATION AND REMOBILIZATION ON TROPONIN T ALTERNATIVE SPLICING

Introduction

Aging (40-42) and skeletal muscle disuse due to immobilization, spinal cord injury (54) and chronic bed rest (53) are some of the leading causes for decreased skeletal muscle strength in humans and have been linked to increased health care costs and mortality risk (43, 44, 88). Previous studies have shown that the decline in muscle function under these conditions is due to loss of muscle mass and decreased force production (45, 55, 56). The molecular mechanisms for these alterations have not been completely elucidated.

In response to mechanical loading of skeletal muscles due to increase in body weight, *Tnnt3* alternative splicing patterns are altered in rat gastrocnemius such that there is increased relative abundance of *Tnnt3* splice forms associated with increased Ca^{2+} sensitivity (18). This enables increased force production by skeletal muscles in order to support the increased body weight. The studies presented in this chapter tested the hypothesis that *Tnnt3* alternative splicing was modified with age. The changes in *Tnnt3* alternative splicing in response to mechanical unloading due to hindlimb immobilization were also determined. In addition, the effects of remobilization after immobilization were studied.

The overall hypothesis is that hindlimb immobilization results in a *Tnnt3* alternative splicing pattern that corresponds to decreased Ca^{2+} sensitivity and remobilization causes restoration of *Tnnt3* alternative splicing patterns to that of normal non-immobilized limbs.

Methods

Animal Studies

The morphological data and muscle samples were obtained from a previous study (46) and are briefly described here. Male Sprague Dawley rats at 2-, 9-, and 18-months of age were obtained from Charles River laboratories and housed under conditions of 12 hour light/dark cycle with *ad libitum* access to standard rodent chow (AIN-93M) and water. Unilateral hindlimb immobilization was carried out by application of a fiberglass cast to one hindlimb as previously described. All immobilized rats were casted for 7 days. One group of 9-month old rats was subjected to a 7-day immobilization period followed by a 7-day remobilization period after cast removal. Prior to tissue harvesting, all rats were fasted overnight (18 hours) with *ad libitum* access to water alone and then fed standard rodent chow for 10 minutes. The gastrocnemius muscle was harvested from anesthetized rats, weighed, frozen between aluminum blocks pre-cooled in liquid nitrogen, and stored at -80˚C prior to analysis. In all experiments, the muscle from the contralateral non-immobilized hindlimb was analyzed as the control. All animal protocols were reviewed and approved by the Institutional Animal Care and Use Committee of the Penn State College of Medicine.

Statistical Analyses

The effects of age on *Tnnt3* splice form relative abundance were evaluated using one-way ANOVA over the three age groups. Multiple comparison error rates were controlled with Tukey's post-hoc test. The effect of immobilization and interaction with age were determined using a two-way nested random effects model (two-way nested ANOVA) to analyze *Tnnt3* splice form relative abundance in the immobilized limb relative to the contralateral non-immobilized limb. The nested random effects model analyzes the relative abundance of the *Tnnt3* splice forms by nesting the limb (immobilized or non-immobilized) within the animal to control for between animal heterogeneity by considering each animal as an experimental unit. Comparisons between immobilized and non-immobilized muscles or remobilized and non-immobilized muscles from the same animal were performed using paired Student's t-test. Statistical significance was set at $p<0.05$. Data are represented as mean ± SEM.

Results

Effects of age on *Tnnt3* alternative splicing

The age of the animals used in this study was chosen based on results of a previous study (89). Thus, 2-month old rats were selected as representative of young growing animals, 9-month old rats as representative of mature adults, and 18-month old rats were selected because age-related loss of muscle mass begins to manifest at approximately this age. In agreement with the earlier study, the relative mass (i.e. muscle mass/body mass ratio) of the gastrocnemius was not different in 2- and 9-month old rats, but was 14% ($p<0.05$) lower in 18-month compared to 9-month old rats (note that both

gastrocnemius and body mass data for the animals used in the present study has been previously reported (46)).

Significant differences were observed in the relative abundance of 10 out of 12 *Tnnt3* splice forms among the three age groups (Table 3.1). The overall pattern of Tnnt3 alternative splicing was such that with increase in age, the relative abundance of all 3 *Tnnt3α* splice forms and 7 *Tnnt3β* splice forms increased and decreased respectively. As illustrated in Figure 3.1A, the total relative abundance of *Tnnt3α* splice forms in gastrocnemius muscles exhibited a continuous increase in expression from 2- to 18-months of age whereas the total relative abundance of *Tnnt3β* splice forms exhibited the opposite pattern of change, i.e. there was a decline in total relative abundance with increasing age (Figure 3.1B). Principal component analysis revealed that the first two principal components (PC1 and PC2) accounted for 97% (PC1 and PC2 captured 74.5% and 22.5%, respectively) of the variation in the dataset. PC1 captured most of the variation in the entire dataset and was significantly affected by age (Table 3.1).

Effects of immobilization on *Tnnt3* alternative splicing

A subset of 2, 9, and 18-month old rats was subjected to 7 days of unilateral hindlimb immobilization (46). As shown in Table 3.2, *Tnnt3* splice form relative abundance in gastrocnemius muscles was altered in response to both age and immobilization. The overall effect of immobilization was decreased relative abundance of all 3 *Tnnt3α* splice forms and increased relative abundance of all 9 *Tnnt3β* splice forms. The total relative abundance of *Tnnt3α* splice forms (Figure 3.2A) was significantly decreased and the total relative abundance of *Tnnt3β* splice forms (Figure 3.2B) was significantly increased in the immobilized limb of 2-, 9- and 18-month old rats

when compared to the control non-immobilized limb of the same animal. Similar to results observed in control, non-immobilized rats, PC1 and PC2 accounted for 97% (88.6% and 8.4%, respectively) of the variation in the dataset. PC1 captured most of the variation in the entire dataset and was significantly affected by both age and immobilization (Table 3.2). Two-way nested ANOVA indicated a significant interaction effect for age and immobilization (Table 3.2). The decrease in total relative abundance of *Tnnt3α* splice forms in response to immobilization in 9- and 18-month old rats (64% and 57% decrease respectively) was greater than in 2-month old rats (35% decrease; one-way ANOVA over the three age groups and Tukey's post-hoc test, $p<0.05$). Similarly, the immobilization-induced change in total relative abundance of *Tnnt3β* splice forms was greater in 18-month old rats (163% increase) than in 2- or 9-month old rats (14% or 29% increase respectively; one-way ANOVA over the three age groups and Tukey's post-hoc test, $p<0.05$).

Effects of immobilization followed by remobilization on *Tnnt3* alternative splicing

To assess the effect of remobilization on *Tnnt3* pre-mRNA alternative splicing, a separate group of 9-month old rats was subjected to unilateral hindlimb immobilization for 7 days after which the cast was removed and the animals were allowed to recover for 7 days (46). This 'Remobilization' group was compared to the 'Immobilization' group that included 9-month old rats casted for 7 days. Similar to results presented in Fig. 3.2, immobilization resulted in decreased total relative abundance of *Tnnt3α* splice forms (Figure 3.3A) and increased total relative abundance of *Tnnt3β* splice forms (Figure 3.3B). Remobilization was associated with an increase in *Tnnt3α* (Figure 3.3A) and a decrease in *Tnnt3β* (Figure 3.3B) splice form total relative abundance, when compared to

the immobilized hindlimb. However, the response to remobilization varied among specific splice forms, with some exhibiting complete restoration to the relative abundance observed in the control non-immobilized hindlimb (e.g. *Tnnt3α3* (Figure 3.3C) and *Tnnt3β8* (Figure 3.3D)), some exhibiting partial restoration (e.g. *Tnnt3α1* (Figure 3.3E)), and others exhibiting no change when compared to the immobilized hindlimb (e.g. *Tnnt3β5* (Figure 3.3F)).

Discussion

Alternative splicing of the *Tnnt3* pre-mRNA in rat gastrocnemius muscle is adjusted to body weight variation associated with normal growth in a precise and quantitative fashion (18). This adjustment depends on the weight that the muscle experiences *per se*, as artificial increases in body weight by means of externally attached loads had the same effect on *Tnnt3* alternative splicing as an equal change in actual body weight. However, the heaviest rats examined in the previous study weighed less than 350 g, and thus the body weight of the youngest rats used in the present study was similar to that of the oldest rats used in the previous study. The present study extends the earlier one and shows that total relative abundance of *Tnnt3α* splice forms associated with increased Ca^{2+} sensitivity significantly increases and total relative abundance of *Tnnt3β* splice forms associated with decreased Ca^{2+} sensitivity decreases in older, heavier rats. Indeed, in younger, lighter rats, *Tnnt3β* splice forms accounted for >80% of *Tnnt3*, whereas in older, heavier rats, *Tnnt3β* splice form relative abundance was reduced to <40% of *Tnnt3*. Moreover, the adjustments to gastrocnemius muscle *Tnnt3* pre-mRNA alternative splicing correlated with body weight despite a significant decrease in relative gastrocnemius mass with age (i.e. at 18-months of age) observed in these animals (46).

Thus, the mechanism that controls body weight dependence, rather than muscle mass dependence, of *Tnnt3* pre-mRNA alternative splicing appears to operate across a much wider range of body weights than reported previously (18), that is, from rats weighing less than 100 g to more than 600 g. It can be inferred that these adjustments to *Tnnt3* pre-mRNA alternative splicing represent the output of a compensatory, body weight-sensitive mechanism that is activated in an attempt to (at least partially) maintain Ca^{2+} sensitivity and muscle force production in the face of reduced muscle mass.

A recent human study showed that in skeletal muscles of elderly male subjects (68 years), *Tnnt3* alternative splicing patterns associated with decreased Ca^{2+} sensitivity were impaired muscle function when compared to young subjects (27 years) even though body weight and lean mass was the same among the individuals of the two age groups (50). On the contrary, in the rat studies discussed in this chapter, increase in age resulted in *Tnnt3* alternative splicing patterns associated with increased Ca^{2+} sensitivity in gastrocnemius muscles. In addition, the body weight dependence of *Tnnt3* alternative splicing was not disrupted in these rats. Although the oldest rats from the study discussed in this chapter (18-month old rats) exhibited deceased relative muscle mass, this age group represented the early stages of aging-related loss of muscle mass (89). This could explain the discrepancy between the present rat studies and the previous human studies. Further studies on rats of higher age groups (>18 months old) are necessary to elucidate the detrimental effects of age on *Tnnt3* alternative splicing.

Previous studies show that hindlimb suspension leads to differential expression of TNNT3 protein isoforms in the soleus muscle (59, 60). In the present study, unilateral hindlimb immobilization dramatically altered the relative abundance of *Tnnt3* splice

forms in the gastrocnemius muscle such that there was a decrease in relative abundance of *Tnnt3α* splice forms associated with increased Ca^{2+} sensitivity and an increase in relative abundance of *Tnnt3β* splice forms associated with decreased Ca^{2+} sensitivity. Indeed, *Tnnt3* pre-mRNA alternative splicing patterns in the immobilized hindlimb muscle were similar to that observed in much younger, lighter rats, with an overall decrease in total relative abundance of *Tnnt3α* splice forms and increased total relative abundance of *Tnnt3β* splice forms compared to non-immobilized hindlimbs. For example, the relative abundance of the *Tnnt3α3* splice form in the gastrocnemius of the immobilized hindlimb from 18-month old rats (mean body weight 538±21 g) was the same as that of the non-immobilized hindlimb gastrocnemius of 2-month old rats (mean body weight 321±5 g). In addition, the effects of immobilization were worsened with age, i.e. the change in total relative abundance of *Tnnt3α* and *Tnnt3β* splice forms was greater in older rats when compared to younger rats. These findings are in parallel with previous human studies that have determined the increased susceptibility of aged skeletal muscles to mechanical unloading (63, 64). While this was not tested specifically, this difference in *Tnnt3* alternative splicing between the immobilized and non-immobilized hindlimbs likely contributes to a decrease in contractility and force production in the atrophied muscles, given the known effects of *Tnnt3α* and *β* splice forms on muscle calcium sensitivity (24). In contrast, after a 7 day recovery period, the pattern of *Tnnt3* pre-mRNA alternative splicing was partially restored to that observed in the non-immobilized hindlimb. Interestingly, although the recovery of *Tnnt3* pre-mRNA alternative splicing patterns started within 7 days of remobilization, gastrocnemius muscle mass had not yet begun to recover (46). Indeed, muscle mass continued to

decline during the recovery period in these animals. Therefore, the remobilization-induced changes in *Tnnt3* pre-mRNA alternative splicing may be an important component in restoration of muscle contractility and performance prior to restoration of mass, and controlled by intracellular pathways independent of those that control muscle mass.

Age and inactivity-related changes in pre-mRNA alternative splicing have been reported for other genes. For example, aging impairs mechanical strain-induced alternative splicing of the insulin-like growth factor I pre-mRNA (40, 90). In muscles of older compared to younger animals, the expression of an insulin-like growth factor I splice variant referred to as mechano growth factor (MGF) is diminished. Moreover, muscle atrophy due to inactivity in animals subjected to hindlimb suspension is associated with changes in alternative splicing of the peroxisome proliferator-activated receptor Gamma Coactivator 1- α (PGC-1α) pre-mRNA, an important regulator of expression of genes involved in energy production in skeletal muscle (91). Whether or not such alterations occur through mechanisms similar to or distinct from the ones involved in controlling *Tnnt3* pre-mRNA alternative splicing is currently unknown. The studies presented in this chapter provide further evidence for the existence of a mechanism(s) that converts quantitative information regarding body weight into appropriate adjustments to muscle sarcomere gene regulation and also suggests that mechanisms controlling sarcomere composition may respond more quickly than those controlling overall muscle mass adjustments to re-loading after a period of disuse.

Figure 3.1: Effects of age on *Tnnt3* alternative splicing

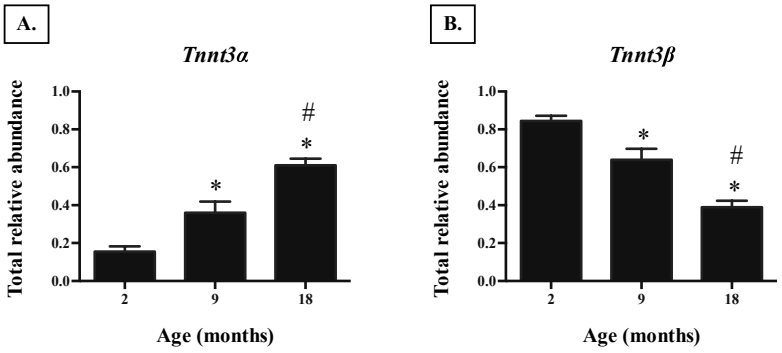

The total relative abundance of (A) *Tnnt3α* and (B) *Tnnt3β* splice forms in gastrocnemius muscle of 2-, 9-, and 18-month old rats is shown. Statistical significance ($p<0.05$) was determined by one-way ANOVA and Tukey's post-hoc test.

n=6-7 per group. * compared to 2-month old rats; # compared to 9-month old rats.

Figure 3.2: Effects of immobilization on *Tnnt3* alternative splicing

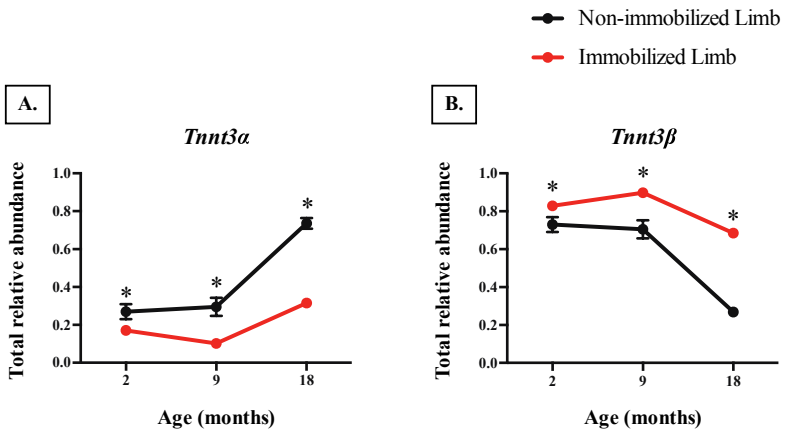

The total relative abundance of (A) *Tnnt3α* and (B) *Tnnt3β* splice forms in gastrocnemius muscle in the immobilized (red circles) and contralateral non-immobilized (black circles) hindlimbs of 2-, 9-, and 18-month old rats is shown. Statistical significance ($p<0.05$) was determined by paired Student's t-test.

n=6-7 per group. * compared to the contralateral non-immobilized limb for that particular age group.

Figure 3.3: Effects of immobilization followed by remobilization on *Tnnt3* alternative splicing

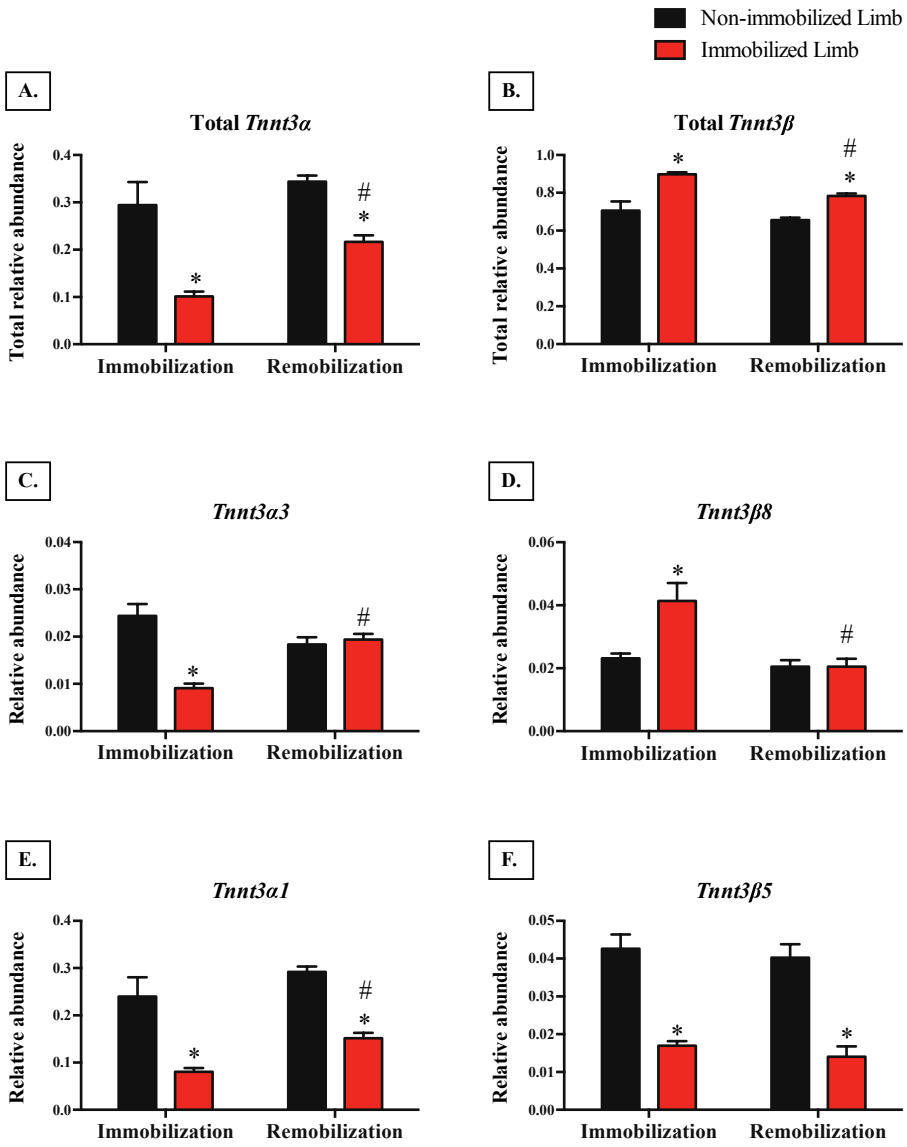

The effect of 7 days of remobilization following 7 days of immobilization on the total relative abundance of (A) *Tnnt3α* and (B) *Tnnt3β* splice form abundance was assessed. The relative abundance of (C) *Tnnt3α3*, (D) *Tnnt3β8*, (E) *Tnnt3α1*, and (F) *Tnnt3β5* are also shown. Statistical significance ($p<0.05$) was determined by Student's t-test.

n=5-6 per group. * compared to the contralateral non-immobilized limb, paired test; # compared to the immobilized limb of the 'Immobilization' group, unpaired test.

Table 3.1: Effects of age on *Tnnt3* alternative splicing

Tnnt3 splice forms	Relative abundance			Effect of Age One-way ANOVA	
	2-month	9-month	18-month	F statistic	p value
α1	0.120 ± 0.024	0.305 ± 0.052 *	0.509 ± 0.033 *#	26.01	< 0.0001
α2	0.020 ± 0.003	0.037 ± 0.006	0.072 ± 0.003 *#	35.52	< 0.0001
α3	0.016 ± 0.001	0.019 ± 0.001	0.029 ± 0.002 *#	24.04	< 0.0001
β1	0.020 ± 0.002	0.008 ± 0.001 *	0.005 ± 0.001 *	23.21	< 0.0001
β2	0.009 ± 0.001	0.008 ± 0.001	0.014 ± 0.002 #	4.985	0.0198
β3	0.360 ± 0.023	0.371 ± 0.048	0.264 ± 0.022	2.731	0.0936
β4	0.023 ± 0.005	0.034 ± 0.007	0.017 ± 0.003	2.326	0.1279
β5	0.084 ± 0.013	0.015 ± 0.006 *	0.003 ± 0.001 *	25.99	< 0.0001
β6	0.084 ± 0.004	0.055 ± 0.010 *	0.045 ± 0.005 *	8.911	0.0023
β7	0.120 ± 0.011	0.047 ± 0.011 *	0.025 ± 0.003 *	27.84	< 0.0001
β8	0.044 ± 0.007	0.023 ± 0.005 *	0.004 ± 0.001 *	15.43	0.0003
β9	0.119 ± 0.015	0.034 ± 0.010 *	0.013 ± 0.002 *	25.59	< 0.0001
Total *Tnnt3α*	0.156 ± 0.028	0.361 ± 0.059 *	0.611 ± 0.035 *#	28.86	< 0.0001
Total *Tnnt3β*	0.844 ± 0.028	0.640 ± 0.059 *	0.389 ± 0.035 *#	28.86	< 0.0001
PC1		*	*#	24.95	< 0.0001
PC2				0.3716	0.6958

The mean ± S.E.M relative abundance of the *Tnnt3* splice forms in gastrocnemius muscle of 2-, 9-, and 18-month old rats is presented. The first two principal components and the results from one-way ANOVA for age effects are shown. Statistically significant differences ($p<0.05$) determined by Tukey's post-hoc testing are indicated.

n=6-7 per group. * compared to 2-month old rats; # compared to 9-month old rats

Table 3.2: Effects of age and immobilization on *Tnnt3* alternative splicing

Tnnt3 splice form	Relative Abundance					
	2-month		9-month		18-month	
	Control limb	Immobilized limb	Control limb	Immobilized limb	Control limb	Immobilized limb
α1	0.197 ± 0.033	0.114 ± 0.018 *	0.240 ± 0.040	0.080 ± 0.008 *	0.586 ± 0.026	0.274 ± 0.034 *
α2	0.038 ± 0.005	0.031 ± 0.004	0.030 ± 0.007	0.012 ± 0.001	0.093 ± 0.006	0.054 ± 0.007 *
α3	0.028 ± 0.004	0.025 ± 0.004	0.024 ± 0.003	0.009 ± 0.001 *	0.048 ± 0.006	0.027 ± 0.004 *
β1	0.015 ± 0.001	0.019 ± 0.001 *	0.010 ± 0.001	0.013 ± 0.001	0.004 ± 0.001	0.006 ± 0.001 *
β2	0.018 ± 0.002	0.017 ± 0.002	0.013 ± 0.003	0.006 ± 0.001	0.022 ± 0.004	0.015 ± 0.002
β3	0.322 ± 0.017	0.315 ± 0.013	0.340 ± 0.026	0.467 ± 0.019	0.162 ± 0.010	0.378 ± 0.028 *
β4	0.029 ± 0.003	0.081 ± 0.009 *	0.023 ± 0.006	0.074 ± 0.017 *	0.010 ± 0.002	0.051 ± 0.007 *
β5	0.054 ± 0.008	0.025 ± 0.002 *	0.038 ± 0.005	0.017 ± 0.001 *	0.005 ± 0.001	0.004 ± 0.001
β6	0.088 ± 0.007	0.108 ± 0.005 *	0.062 ± 0.006	0.105 ± 0.004 *	0.032 ± 0.004	0.092 ± 0.008 *
β7	0.096 ± 0.006	0.099 ± 0.006	0.081 ± 0.015	0.097 ± 0.010	0.019 ± 0.002	0.052 ± 0.004 *
β8	0.034 ± 0.006	0.054 ± 0.006 *	0.023 ± 0.002	0.041 ± 0.006 *	0.004 ± 0.001	0.013 ± 0.002 *
β9	0.098 ± 0.011	0.110 ± 0.006	0.056 ± 0.008	0.077 ± 0.005 *	0.015 ± 0.002	0.034 ± 0.003 *
Total *Tnnt3α*	0.171 ± 0.026	0.269 ± 0.040 *	0.102 ± 0.010	0.294 ± 0.049 *	0.316 ± 0.025	0.736 ± 0.028 *
Total *Tnnt3β*	0.829 ± 0.026	0.731 ± 0.040 *	0.898 ± 0.010	0.706 ± 0.049 *	0.684 ± 0.025	0.268 ± 0.025 *

Tnnt3 splice form	Two-way ANOVA (nested model)					
	Effect of Age		Effect of Immobilization		Age * Immobilization	
	F statistic	p value	F statistic	p value	F statistic	p value
α1	65.1542	<0.0001	52.5714	<0.0001	10.7655	0.0003
α2	44.7273	<0.0001	19.4619	0.0001	4.8226	0.0153
α3	9.9045	0.0005	13.0311	0.0011	2.4487	0.1035
β1	76.5313	<0.0001	11.5078	0.002	0.1905	0.8275
β2	5.2331	0.0112	4.237	0.0483	0.7098	0.4998
β3	30.0513	<0.0001	31.4339	<0.0001	19.5423	<0.0001
β4	6.8984	0.0034	61.1599	<0.0001	0.3459	0.7104
β5	38.6427	<0.0001	21.6376	<0.0001	6.1588	0.0057
β6	19.8269	<0.0001	60.6869	<0.0001	5.9859	0.0065
β7	54.4016	<0.0001	9.0167	0.0054	2.8995	0.0706
β8	38.1622	<0.0001	17.4841	0.0002	0.9474	0.3991
β9	79.9899	<0.0001	9.757	0.0039	0.2294	0.7964
Total *Tnnt3α*	62.8523	<0.0001	49.4036	<0.0001	10.2252	0.0004
Total *Tnnt3β*	65.0894	<0.0001	51.161	<0.0001	10.5915	0.0003
PC1	60.6813	<0.0001	54.0919	<0.0001	13.224	<0.0001
PC2	33.7262	<0.0001	0.9318	0.3421	8.3441	0.0013

The mean ± S.E.M relative abundance of the *Tnnt3* splice forms in gastrocnemius muscle from immobilized and contralateral non-immobilized (control) limbs of 2-, 9-, and 18-month old rats is presented. The first two principal components and the results from two-way nested ANOVA for age, immobilization and interaction (Age * Immobilization) effects are shown. Statistically significant changes ($p<0.05$) determined by paired Student's t-test are indicated.

n=6-7 per group. * compared to the control limb for that particular age group.

Chapter 4.

EFFECTS OF HIGH FAT DIET ON TROPONIN T ALTERNATIVE SPLICING

Introduction

Obesity is a widespread disease affecting more than one-third of adults and 17% of children in the United States (66). Obese individuals suffer from severe restrictions to mobility, decreased capacity to perform day-to-day activities and have increased fall risk because of decreased skeletal muscle strength relative to their excessive body mass (69). The molecular mechanisms for this decline in muscle function are not completely understood. Previous studies have determined that in skeletal muscles of insects and mammals, alternative splicing of *TnT* (15, 21) and *Tnnt3* (18) respectively modulates Ca^{2+} sensitivity and force production during muscle contraction. Increase in body weight leads to a quantitative shift in alternative splicing patterns such that relative abundance of *TnT* (in flight muscles of moths) (28) and *Tnnt3* (in gastrocnemius of rats) (18) splice forms associated with increased Ca^{2+} sensitivity is increased, thereby resulting in improved muscle function to support the increased body weight. Moreover, Schilder et al. showed that this body weight dependence of *Tnnt3* alternative splicing is impaired in obese Zucker rats (18).

Obesity is a multifactorial disease caused by several genetic, dietary and environmental factors and one of the primary causes is excessive intake of dietary saturated fatty acids (74, 75). The objective of the studies presented in this chapter is to

elucidate the changes in *Tnnt3* alternative splicing in rat gastrocnemius muscles in response to consumption of a high fat diet (HFD) containing increased amount of saturated fatty acids, as a model for the early stages in the development of obesity. The overall hypothesis is that HFD results in a *Tnnt3* alternative splicing pattern corresponding to decreased Ca^{2+} sensitivity and force production. In addition, it is hypothesized that the linear relationship between body weight and relative abundance of *Tnnt3* splice forms is disrupted in HFD-fed rats.

Methods

Animal Studies

Male obesity-prone Sprague-Dawley rats (OP-CD) were obtained from Charles River laboratories and two different feeding studies were carried out. For the first study, approximately 6-week old rats were placed on reverse 12 hour light/dark cycle (8 am lights off, 8 pm lights on) with *ad libitum* access to water. The rats were fed either control diet (CD – 10 kcal% fat, 70 kcal% carbohydrate and 20 kcal% protein) or high fat diet (HFD – 60 kcal% fat, 20 kcal% carbohydrate and 20 kcal% protein) for 2 weeks. For the first two days of the study, the rats were allowed *ad libitum* access to food in order to allow them to acclimate to the light/dark cycle and the different diets. From the third day onwards until the rest of the study, the rats were fed in a time-restricted manner for 3 hours i.e. from 8 am to 11 am daily. Prior to tissue harvesting, the rats were fed the respective diets for 1 hour. For the second study, approximately 4-week old rats were placed on normal 12 hour light/dark cycle (8 am lights on, 8 pm lights off). The rats were provided either CD or HFD for 8 weeks with *ad libitum* access to food and water.

The gastrocnemius muscle was harvested from anesthetized rats, frozen between aluminum blocks pre-cooled in liquid nitrogen, and stored at -80˚C prior to analysis. All animal protocols were reviewed and approved by the Institutional Animal Care and Use Committee of the Penn State College of Medicine.

Statistical Analyses

The body weights and calorie consumption of HFD-fed rats and relative abundance of *Tnnt3* splice forms in gastrocnemius were compared with that of CD-fed rats using unpaired Student's t-test. The effect of diet and interaction with body weight were determined using a linear regression multivariate model (two-way ANOVA along with regression analysis) to evaluate the linear relationship between relative abundance of *Tnnt3* splice forms and body weight. Statistical significance was set at $p<0.05$. Data are represented as mean ± SEM.

Results

Effects of 2 week consumption of HFD on *Tnnt3* alternative splicing

The initial body weight was similar in both diet groups, i.e. 198 g ± 5.07 (mean ± SEM) for CD group and 199 g ± 5.11 for HFD group. Over the course of the 3 hour time-restricted feeding regimen, the mean calorie consumption of HFD-fed rats (84.1 kcal/day) was higher than that of CD-fed rats (58.3 kcal/day; unpaired Student's t-test, $p<0.0001$). At the end of the 2 week study, the body weight (Figure 4.1A) and weight of epididymal fat pads were higher in HFD-fed rats compared to CD-fed rats (Figure 4.1B). As shown in Table 4.1, the relative abundance of 9 out of 12 Tnnt3 splice forces was altered in response to 2 week HFD feeding. The total relative abundance of *Tnnt3α* splice forms

(Figure 4.1C) increased and that of *Tnnt3β* splice forms (Figure 4.1D) decreased in gastrocnemius muscles of HFD-fed rats when compared to CD-fed rats. Considering the individual splice forms (Table 4.1), it was observed that the relative abundance of all 3 *Tnnt3α* splice forms was decreased and that of 7 *Tnnt3β* splice forms was increased in HFD- compared to CD-fed rats.

Effects of 8 week consumption of HFD on *Tnnt3* alternative splicing

The initial body weight was not significantly different among the two diet groups, i.e. 104 g ± 3.21 (mean ± SEM) for CD group and 109 g ± 3.71 for HFD group. Similar to the time-restricted 2 week feeding studies, the ad libitum HFD-fed rats consumed greater amount of calories daily (163.2 kcal/day) than the ad libitum CD-fed rats (116.4 kcal/day; unpaired Student's t-test, $p<0.0001$). After 8 weeks, the body weights (Figure 4.2A) and fat pad weights (Figure 4.2B) of HFD-fed rats were higher when compared to CD-fed rats. However, no significant differences were observed in the total relative abundance of *Tnnt3α* (Figure 4.2C) and *Tnnt3β* splice forms (Figure 4.2D) among HFD- and CD-fed rats. The relative abundance of only three individual *Tnnt3* splice forms was altered in response to 8 weeks of HFD feeding (Table 4.1). *Tnnt3α3* relative abundance was increased and *Tnnt3β1* and *Tnnt3β6* relative abundances were decreased in HFD-fed rats compared to CD-fed rats.

Effects of body weight and HFD consumption on *Tnnt3* alternative splicing

The *Tnnt3* splice form results from the 2 week and 8 week studies were combined together for the regression analysis. Significant effects of diet and body weight were seen for 9 out of 12 *Tnnt3* splice forms (Table 4.1). No significant effect of interaction was

observed with body weight for any of the splice forms. Principal component analysis indicated that PC1 and PC2 accounted for 96% (77.5% and 18.5%, respectively) of the variation in the dataset. PC1 was significantly affected by both body weight and diet but there was no significant interaction effect.

In CD-fed rats, the total relative abundance of *Tnnt3α* splice forms (Figure 4.3A) increased linearly with body weight. This linear relationship was also seen in HFD-fed rats but the total relative abundance was significantly lower when compared CD-fed rats. The total relative abundance of *Tnnt3β* splice forms (Figure 4.3B) decreased with increase in body weight in both HFD- and CD-fed rats and the HFD-fed rats showed higher total relative abundance compared to CD-fed rats. The slope of the regression lines for *Tnnt3α* (Figure 4.3A) and *Tnnt3β* splice forms (Figure 4.3B) corresponding to HFD- and CD-fed rats were similar as no interaction effect between body weight and diet was seen. The regression plots for effects of body weight and diet on relative abundance of all 3 individual *Tnnt3α* and 6 individual *Tnnt3β* splice forms were similar to figures 4.3A and 4.3B representing the effects observed on total relative abundance of *Tnnt3α* and *Tnnt3β* splices forms respectively (Table 4.2).

Discussion

Schilder et al. demonstrated that the proportionality between body weight and relative abundance of *Tnnt3* splice forms is disrupted in gastrocnemius muscles of obese Zucker rats such that the relative abundance in heavier obese rats is similar to that in lean rats of lower body weight (18). Since obesity is a polygenic disease (74, 75, 92), the results from genetically identical Zucker rats cannot be efficiently linked to the development of obesity in humans. In addition, the phenotype of Zucker rats is similar to

advanced stages of human obesity (93, 94). HFD-induced obesity in rodent models is a more powerful method to study the early stages of obesity caused by increased energy intake, similar to humans (76, 94-97). Previous studies have shown that a subpopulation of Sprague-Dawley rats does not become obese after HFD consumption. So, the rodent model utilized in the study described in this chapter is a polygenic obesity model that is developed from Sprague-Dawley rats by selecting for rats that show increased weight gain and can become insulin resistant upon HFD feeding called obesity-prone rats. According to the Dietary Guidelines for Americans 2010, it is recommended that a balanced diet should contain 20% to 35% of calories from fat and less than 10% of calories from saturated fats (98). The diets used in this study were designed considering these guidelines such that saturated fat from lard accounted for 10% of calories from CD and 60% of calories from HFD. The carbohydrate content is lower in HFD when compared to CD and so, the rats fed HFD consumed more food in order to get the required amount of carbohydrates, similar to previous studies on diets containing different percentages of fat (99). So, the studies in this chapter delineate the effects of increased energy consumption during the early stages of obesity.

The results presented in this chapter indicate that 2 weeks of HFD consumption in a time-restricted manner resulted in abnormal *Tnnt3* alternative splicing. The body weight of HFD-fed rats was significantly higher than CD-fed rats. However, the relative abundance of *Tnnt3* splice forms in gastrocnemius muscles was disproportionate to the increased body weight in HFD-fed rats, and similar to what would be expected in a muscle of a much lighter animal. Thus, the total relative abundance of *Tnnt3α* splice forms (associated with increased Ca^{2+} sensitivity) was decreased and that of *Tnnt3β*

splice forms (associated with decreased Ca^{2+} sensitivity) was increased in HFD-fed rats when compared to CD-fed rats. From these results, it can be inferred that changes in *Tnnt3* alternative splicing caused by 2 weeks of time-restricted HFD feeding lead to decreased Ca^{2+} sensitivity and contributed to decreased force production in gastrocnemius muscles.

In *ad libitum* fed rats, 8 weeks of HFD consumption resulted in aberrant *Tnnt3* alternative splicing. Although the 8 week HFD-fed rats had higher body weight when compared to CD-fed rats, the total relative abundance of *Tnnt3α* splice forms and that of *Tnnt3β* splice forms was not statistically different between HFD- and CD-fed rats. Hence, the relative abundance of *Tnnt3* splice forms in gastrocnemius of heavier HFD-fed rats was similar to lighter CD-fed rats. This mismatch between body weight and *Tnnt3* alternative splicing is similar to the findings of Schilder et al. in obese Zucker rats (18).

The 2 week and 8 week studies described herein consisted of rats of different age groups (initial age approximately 6 weeks and 4 weeks respectively). The initial and final body weights of rats from both studies were within the body weight range of rats in the study by Schilder et al. (18) and in the studies presented in chapter 3 of this thesis. Also, the body weight dependence of *Tnnt3* alternative splicing was present in rats until the age of 18 months (chapter 3 of thesis). Therefore, no detrimental effect of age is expected in the relatively young rats from the 2 week study (initial and final age <2 months) and 8 week study (initial age approximately 1 month and final age approximately 3 months).

HFD-induced changes in *Tnnt3* alternative splicing in both 2 week and 8 week studies was assessed together using linear regression models for dependence of relative abundance of *Tnnt3* splice forms on body weight in order to determine the effect of body

weight and diet. The total relative abundance of *Tnnt3α* splice forms increased linearly with increase in body weight in both HFD- and CD-fed rats, i.e. the slope of the regression lines was not significantly different. The regression analysis was used to define the effect of HFD compared to CD after normalizing for effect of body weight. There was a significant decrease in total relative abundance of *Tnnt3α* splice forms in gastrocnemius of HFD-fed rats when compared to CD-fed rats. The total relative abundance of *Tnnt3β* splice forms had a linear, negative correlation with body weight and there was a significant increase in gastrocnemius of HFD- compared to CD-fed rats. In addition, no significant interaction was seen between the effect of diet and body weight, indicating that HFD-induced changes in *Tnnt3* alternative splicing were independent of body weight and the effects of HFD were similar in the 2 week and 8 week studies.

Marden et al. showed that duration of food restriction affects *Tnnt3* alternative splicing in moths (28). The 2 week studies described herein also included a time-restricted feeding regimen that resulted in body weight-independent effects of diet. Further studies on different time periods of food restriction and longer duration of HFD feeding will be necessary to distinguish between the effect of dietary regimen and HFD.

Previous studies have shown that HFD consumption results in increased plasma concentrations of free saturated fatty acids (79). This excess fatty acid availability along with diminished capacity for fatty acid oxidation in tissues such as liver and skeletal muscles leads to increased accumulation of fatty acids in these tissues. Although plasma and tissue concentrations of fatty acids were not directly measured in the 2 and 8 week studies presented in this chapter, the weight of epididymal fat pads were significantly higher in HFD- (i.e. mean weight was 5 g at 2 weeks and 15 g at 8 weeks) compared to

CD-fed rats (i.e. mean weight was 5 g at 2 weeks and 15 g at 8 weeks; unpaired Student's t-test, $p<0.0001$), indicating excessive fatty acid build-up in these models for early stages of HFD-induced obesity. Fatty acid overload has been linked to insulin resistance in skeletal muscles (77, 79-81). Rodent studies involving HFD feeding (77, 80, 81) and treatment of skeletal muscle cells in culture with saturated fatty acids (78, 79) like palmitate have been shown to result in decreased insulin-stimulated Akt activity. Tremblay et al. showed that phosphorylation status of Akt was not altered in response to HFD feeding but kinase activity towards Akt substrates was decreased (81). This downregulation of Akt activity could be a potential mechanism leading to aberrant *Tnnt3* alternative splicing observed in HFD-fed rats in the studies discussed in this chapter.

Several studies have elucidated the role of dietary saturated fatty acids in regulating alternative splicing of several pre-mRNAs such as XBP1 (X-box-binding protein-1) (100, 101) and GIPR (receptor for glucose-dependent insulinotropic polypeptide) (102, 103) in tissues such as liver, pancreas and adipocytes. However, alternative splicing events in skeletal muscle regulated by fatty acids have not been extensively investigated. The studies discussed in this chapter describe the variation in *Tnnt3* alternative splicing patterns in response to HFD consumption. The changes in *Tnnt3* alternative splicing can be attributed to defective ability of skeletal muscles HFD-fed rats to respond to changes in body weight. In addition, the observed changes in *Tnnt3* alternative splicing are associated with decreased Ca^{2+} sensitivity and force production. This study puts forward a novel mechanism for obesity-related decline in skeletal muscle function involving alterations in sarcomere components during early stages in development of diet-induced obesity.

Figure 4.1: Effects of 2 week HFD consumption on *Tnnt3* alternative splicing

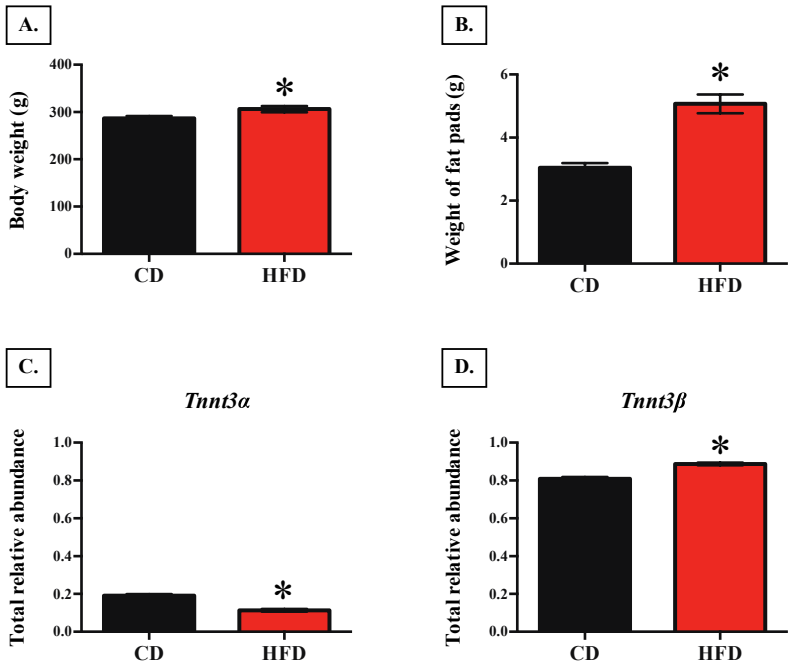

The (A) body weight, (B) weight of fat pads, total relative abundance of (C) *Tnnt3α* and (D) *Tnnt3β* splice forms in gastrocnemius muscle of rats fed CD and HFD for 2 weeks are shown. Statistical significance ($p<0.05$) was determined by unpaired Student's t test. n=11 per diet group. * compared to CD-fed rats

Figure 4.2: Effects of 8 week HFD consumption on *Tnnt3* alternative splicing

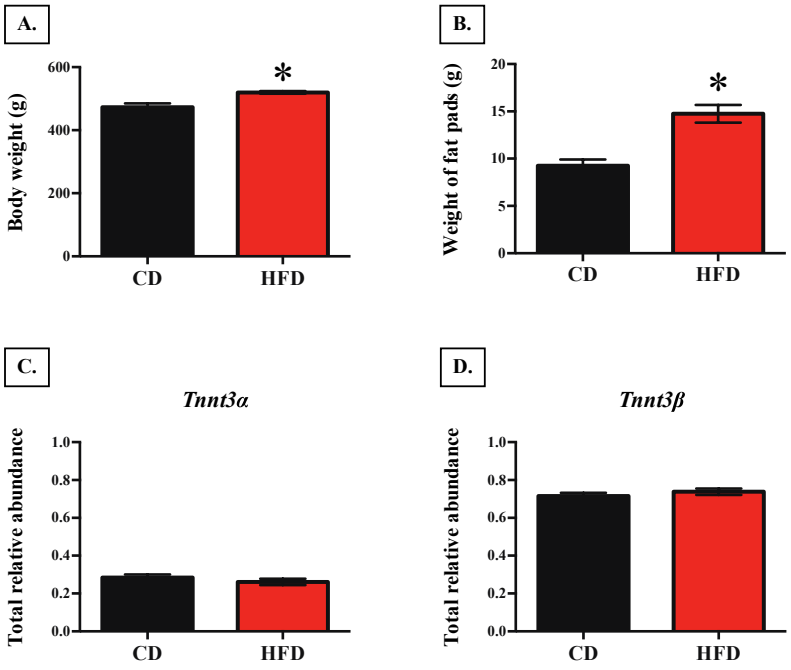

The (A) body weight, (B) weight of fat pads, total relative abundance of (C) *Tnnt3α* and (D) *Tnnt3β* splice forms in gastrocnemius muscle of rats fed CD and HFD for 8 weeks are shown. Statistical significance ($p<0.05$) was determined by unpaired Student's t test. n=7 per diet group. * compared to CD-fed rats

Figure 4.3: Effects of body weight and HFD consumption on *Tnnt3* alternative splicing

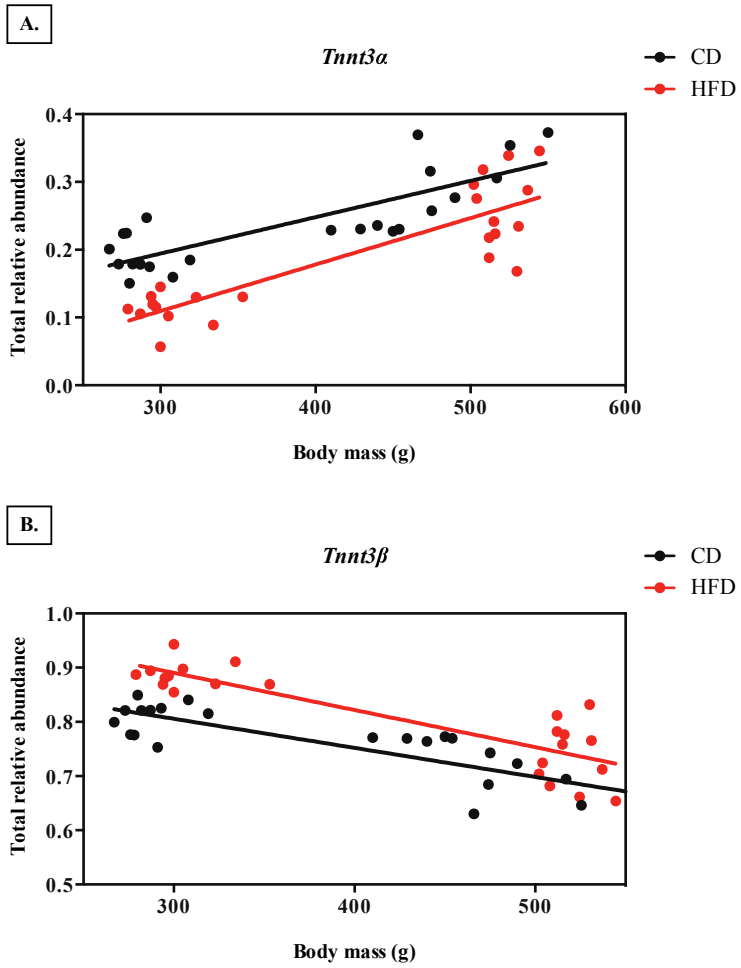

The relationship between body weight and total relative abundance of (A) *Tnnt3α* and (B) *Tnnt3β* splice forms in gastrocnemius muscle of rats fed CD (black circles, black regression line) and HFD (red circles, red regression line) is presented. Statistical significance ($p<0.05$) was determined by two-wat ANOVA with regression analysis.

n= 18 per diet group

Table 4.1: Effects of HFD consumption for 2 and 8 weeks on *Tnnt3* alternative splicing

Tnnt3 splice forms	Effect of 2 week feeding			Effect of 8 week feeding		
	Relative abundance		Unpaired Student's t-test	Relative abundance		Unpaired Student's t-test
	Control Diet	High Fat Diet	p value	Control Diet	High Fat Diet	p value
α1	0.148 ± 0.008	0.082 ± 0.005 *	< 0.0001	0.230 ± 0.014	0.211 ± 0.014	0.3542
α2	0.025 ± 0.001	0.017 ± 0.001 *	< 0.0001	0.035 ± 0.002	0.034 ± 0.002	0.8181
α3	0.019 ± 0.001	0.013 ± 0.001 *	0.0039	0.019 ± 0.001	0.016 ± 0.001 *	0.0174
β1	0.017 ± 0.001	0.019 ± 0.001 *	0.0476	0.012 ± 0.001	0.015 ± 0.001 *	0.0165
β2	0.012 ± 0.001	0.011 ± 0.001	0.3672	0.013 ± 0.001	0.012 ± 0.009	0.4643
β3	0.378 ± 0.009	0.363 ± 0.010	0.2594	0.383 ± 0.011	0.388 ± 0.011	0.7222
β4	0.023 ± 0.001	0.030 ± 0.002 *	0.0026	0.029 ± 0.002	0.0289 ± 0.002	0.8029
β5	0.075 ± 0.004	0.087 ± 0.008	0.1765	0.048 ± 0.003	0.055 ± 0.007	0.3232
β6	0.080 ± 0.002	0.089 ± 0.003 *	0.0386	0.071 ± 0.002	0.077 ± 0.002 *	0.0358
β7	0.092 ± 0.003	0.113 ± 0.003 *	< 0.0001	0.063 ± 0.003	0.059 ± 0.003	0.4629
β8	0.040 ± 0.002	0.054 ± 0.005 *	0.0201	0.035 ± 0.002	0.0363 ± 0.003	0.7291
β9	0.092 ± 0.003	0.122 ± 0.005 *	0.0001	0.062 ± 0.002	0.0664 ± 0.005	0.4375
Total *Tnnt3α*	0.191 ± 0.009	0.112 ± 0.007 *	< 0.0001	0.284 ± 0.017	0.261 ± 0.017	0.3521
Total *Tnnt3β*	0.809 ± 0.009	0.888 ± 0.007 *	< 0.0001	0.716 ± 0.017	0.739 ± 0.017	0.3521

The mean ± S.E.M relative abundance of the *Tnnt3* splice forms in gastrocnemius muscle of rats fed CD or HFD for 2 and 8 weeks is presented. Statistically significant differences ($p<0.05$) determined by unpaired Student's t-test are indicated.

n=11-12 per diet group. * compared to CD-fed rats

Table 4.2: Effects of body weight and high fat diet on *Tnnt3* alternative splicing

Tnnt3 splice form	Two-way ANOVA (linear regression model)					
	Effect of Diet		Effect of Body Weight		Diet * Body weight	
	F statistic	p value	F statistic	p value	F statistic	p value
α1	30.7852	<0.0001	108.7549	<0.0001	1.5675	0.2175
α2	13.713	0.0006	71.2303	<0.0001	0.969	0.3306
α3	19.5493	<0.0001	3.1704	0.0822	0.2731	0.604
β1	18.4333	0.0001	44.3835	<0.0001	0.7906	0.379
β2	1.7935	0.1877	1.1277	0.2943	0.0092	0.9239
β3	0.3105	0.5803	0.627	0.4329	1.8729	0.1784
β4	1.9155	0.1737	1.5023	0.2271	3.6505	0.0629
β5	6.1583	0.0172	24.4363	<0.0001	0.0001	0.9913
β6	14.3443	0.0005	19.6894	<0.0001	0.0246	0.8762
β7	27.2532	<0.0001	203.873	<0.0001	11.2151	0.0017
β8	7.9101	0.0074	11.4421	0.0016	3.1992	0.0809
β9	30.5105	<0.0001	98.861	<0.0001	6.6591	0.0135
Total *Tnnt3α*	30.5918	<0.0001	101.6743	<0.0001	1.5157	0.2251
Total *Tnnt3β*	30.5918	<0.0001	101.6743	<0.0001	1.5157	0.2251
PC1	34.3313	<0.0001	125.4452	<0.0001	2.7845	0.1026
PC2	0.0011	0.9735	0.0202	0.8876	1.0568	0.3098

The results from regression analysis (two-way ANOVA with a linear regression model) for diet, body weight and interaction (Diet * Body weight) effects on relative abundance of the *Tnnt3* splice forms in gastrocnemius muscle from CD- and HFD-fed rats are presented. The first two principal components are shown. Statistically significant changes ($p<0.05$) determined by post-hoc analyses are indicated.

n=18 per diet group.

Chapter 5.

SUMMARY AND FUTURE PERSPECTIVES

The goal of the studies presented this thesis was to determine variations in *Tnnt3* alternative splicing patterns in gastrocnemius muscles in response to different conditions of impaired skeletal muscle function – aging, immobilization and HFD-induced obesity. It was hypothesized that under these conditions, there is decreased relative abundance of *Tnnt3* splice forms that have been associated with increased Ca^{2+} sensitivity and increased relative abundance of *Tnnt3* splice forms that have been associated with decreased Ca^{2+} sensitivity. This will result in an overall decrease in Ca^{2+} sensitivity of gastrocnemius muscle fibers leading to decreased activation of cross-bridges even in the presence of Ca^{2+} and decreased force production during muscle contraction.

The results presented in this thesis provide further evidence regarding the relationship between body weight and *Tnnt3* alternative splicing. In the studies in chapter 2, relative abundance of *Tnnt3* splice forms in gastrocnemius muscles of Sprague-Dawley rats of three different age groups (2, 9 and 18 months old) was proportionate to body weight even though decreased relative muscle mass was observed in the older rats due to aging-related skeletal muscle atrophy. 7-day hindlimb immobilization resulted in a *Tnnt3* alternative splicing pattern predicted to result in decreased Ca^{2+} sensitivity and force production. In addition, immobilization had greater effects on *Tnnt3* alternative splicing in the older rats. A major finding in these studies is that remobilization following hind limb immobilization lead to restoration of *Tnnt3* alternative splicing to near-normal

patterns in spite of a sustained decrease in muscle mass. Therefore, it can be inferred that muscle mass and muscle function are regulated by independent molecular mechanisms and the latter is coordinated by body weight sensing signaling pathways that modulate sarcomere components.

The studies described in chapter 3 were aimed at determining the changes in *Tnnt3* alternative splicing caused by excessive consumption of dietary saturated fatty acids. HFD feeding for 2 and 8 weeks resulted in a *Tnnt3* alternative splicing pattern that is disproportionate to body weight and associated with decreased Ca^{2+} sensitivity and force production. This HFD-induced obesity model corresponds to early stages of obesity i.e. before the development of significant hyperglycemia, skeletal muscle atrophy and insulin resistance (76). Therefore, the changes in *Tnnt3* alternative splicing observed in these studies can be attributed to direct effects of increased saturated fatty acid intake on skeletal muscles resulting in inability to modulate muscle function according to body weight. This imbalance in body weight sensing mechanisms can be considered as early changes in the development of obesity.

Future directions

The gastrocnemius is the primary weight-bearing muscle and so the studies discussed in this thesis were focused on this muscle (29). Since *Tnnt3* is expressed only by fast skeletal muscle fibers (5) and gastrocnemius consists of almost equal proportions of fast and slow fibers (30, 104), it is important to look at changes in *Tnnt3* alternative splicing in other muscles composed primarily of fast fibers such as plantaris, extensor digitorum longus and tibialis anterior (30).

Previous studies that elucidated the functions of *Tnnt3* splice forms were mostly dependent on *in vitro* binding assays to determine the affinities for Tm, TnC and TnI (23, 25, 26). Ca^{2+} sensitivity was assessed by reconstitution of isolated single muscle fibers with some of the *Tnnt3* splice forms (24). Some studies have looked at Ca^{2+} sensitivity and force production of intact muscles (15, 21, 28), but these studies have only correlated relative abundance of some *TnT* splice forms with changes in muscle function. So, future studies involving transfection of different types of muscles containing fast muscle fibers like gastrocnemius and plantaris to enable expression of a particular splice form or groups of splice forms will contribute to determining the effect of individual *Tnnt3* splice forms on whole muscle performance.

Since TnT is an important regulator of muscle function, future studies should be directed at the molecular mechanisms for the regulation of *Tnnt3* alternative splicing. A few studies have shown that Akt (32) and muscleblind (35) signaling pathways are involved but the downstream effectors involved in the direct effects on *Tnnt3* alternative splicing have not yet been established. Down-regulation of Akt acitivity has been observed in response to aging (51), skeletal muscle disuse (61) and HFD feeding (81). The potential role of Akt in regulating *Tnnt3* alternative splicing under these conditions needs to be elucidated. In addition, the understanding of splicing events in skeletal muscles is very limited. Akt has been shown to activate and phosphorylate splicing factors (105) like SRp40 that has been linked to regulation of alternative splicing of protein kinase C pre-mRNA in skeletal muscle cells in response to insulin (31). Skeletal muscle-specific splicing factors like Rbfox family of proteins have been shown to regulate alternative splicing of several pre-mRNAs (106). Similarly, splicing factors

involved in *Tnnt3* pre-mRNA processing need to be identified and their regulation by Akt signaling needs to be determined.

***Troponin T* alternative splicing in physiological conditions**

Skeletal muscle function is a fundamental predictor of overall behavior, movement and efficiency in performing a wide range of activities (43, 69). Changes in *TnT* alternative splicing has been linked to decreased activity and sedentary behavioral changes in butterflies (28). Similar mechanisms could be involved in decreased physical activity and lack of motivation to exercise seen in obese individuals (71).

Aging (48) and obesity (67) are associated with several co-morbidities such as diabetes and cardiovascular diseases. Most health care efforts are focused on treating these co-morbidities and there is relatively less emphasis on tackling the decline in skeletal muscle function that leads to decreased quality of life (48, 66). In addition, current therapeutic strategies to improve muscle function such as dietary protein and amino acid supplementation are not effective for aged or obese individuals (107). So, there is a significant demand for novel therapeutic interventions to enhance muscle performance. The findings presented in this thesis provide a better understanding of molecular changes in skeletal muscles during conditions of decreased muscle function. Such studies on changes in sarcomere components will be instrumental in designing therapeutic approaches for preventing or mitigating decline in skeletal muscle function seen in various physiological conditions like aging, immobilization, obesity and cancer.

Chapter 6.

REFERENCES

(1) Coelho MB, Smith CW. Regulation of alternative pre-mRNA splicing. *Methods Mol Biol* 2014;1126:55-82. 10.1007/978-1-62703-980-2_5

(2) Chen M, Manley JL. Mechanisms of alternative splicing regulation: insights from molecular and genomics approaches. *Nat Rev Mol Cell Biol* 2009;10:741-54. 10.1038/nrm2777

(3) Zhou Z, Fu XD. Regulation of splicing by SR proteins and SR protein-specific kinases. *Chromosoma* 2013;122:191-207. 10.1007/s00412-013-0407-z

(4) Salati LM, Szeszel-Fedorowicz W, Tao H, Gibson MA, Amir-Ahmady B, Stabile LP, Hodge DL. Nutritional regulation of mRNA processing. *J Nutr* 2004;134:2437S-43S.

(5) Perry SV. Troponin T: genetics, properties and function. *J Muscle Res Cell Motil* 1998;19:575-602.

(6) Kornblihtt AR, Schor IE, Alló M, Dujardin G, Petrillo E, Muñoz MJ. Alternative splicing: a pivotal step between eukaryotic transcription and translation. *Nat Rev Mol Cell Biol* 2013;14:153-65. 10.1038/nrm3525

(7) Matsakas A, Patel K. Skeletal muscle fibre plasticity in response to selected environmental and physiological stimuli. *Histol Histopathol* 2009;24:611-29.

(8) Guellich A, Negroni E, Decostre V, Demoule A, Coirault C. Altered cross-bridge properties in skeletal muscle dystrophies. *Front Physiol* 2014;5:393. 10.3389/fphys.2014.00393

(9) Månsson A, Rassier D, Tsiavaliaris G. Poorly Understood Aspects of Striated Muscle Contraction. *Biomed Res Int* 2015;2015:245154. 10.1155/2015/245154

(10) GM C. The Cell: A Molecular Approach ed. Sunderland (MA): Sinauer Associates; 2000. 0-87893-106-6. url: http://www.ncbi.nlm.nih.gov/books/NBK9961/

(11) Gomes AV, Potter JD, Szczesna-Cordary D. The role of troponins in muscle contraction. *IUBMB Life* 2002;54:323-33. 10.1080/15216540216037

(12) Ferrante MI, Kiff RM, Goulding DA, Stemple DL. Troponin T is essential for sarcomere assembly in zebrafish skeletal muscle. *J Cell Sci* 2011;124:565-77. 10.1242/jcs.071274

(13) Farah CS, Reinach FC. The troponin complex and regulation of muscle contraction. *FASEB J* 1995;9:755-67.

(14) Reinach FC, Farah CS, Monteiro PB, Malnic B. Structural interactions responsible for the assembly of the troponin complex on the muscle thin filament. *Cell Struct Funct* 1997;22:219-23.

(15) Marden JH, Fitzhugh GH, Wolf MR, Arnold KD, Rowan B. Alternative splicing, muscle calcium sensitivity, and the modulation of dragonfly flight performance. *Proc Natl Acad Sci U S A* 1999;96:15304-9.

(16) Medford RM, Nguyen HT, Destree AT, Summers E, Nadal-Ginard B. A novel mechanism of alternative RNA splicing for the developmentally regulated generation of troponin T isoforms from a single gene. *Cell* 1984;38:409-21.

(17) Ogut O, Granzier H, Jin JP. Acidic and basic troponin T isoforms in mature fast-twitch skeletal muscle and effect on contractility. *Am J Physiol* 1999;276:C1162-70.

(18) Schilder RJ, Kimball SR, Marden JH, Jefferson LS. Body weight-dependent troponin T alternative splicing is evolutionarily conserved from insects to mammals and is partially impaired in skeletal muscle of obese rats. *J Exp Biol* 2011;214:1523-32. 10.1242/jeb.051763

(19) Briggs MM, Schachat F. Physiologically regulated alternative splicing patterns of fast troponin T RNA are conserved in mammals. *Am J Physiol* 1996;270:C298-305.

(20) Stefancsik R, Randall JD, Mao C, Sarkar S. Structure and sequence of the human fast skeletal troponin T (TNNT3) gene: insight into the evolution of the gene and the origin of the developmentally regulated isoforms. *Comp Funct Genomics* 2003;4:609-25. 10.1002/cfg.343

(21) Marden JH, Fitzhugh GH, Girgenrath M, Wolf MR, Girgenrath S. Alternative splicing, muscle contraction and intraspecific variation: associations between troponin T transcripts, Ca(2+) sensitivity and the force and power output of dragonfly flight muscles during oscillatory contraction. *J Exp Biol* 2001;204:3457-70.

(22) Schachat FH, Diamond MS, Brandt PW. Effect of different troponin T-tropomyosin combinations on thin filament activation. *J Mol Biol* 1987;198:551-4.

(23) Chaudhuri T, Mukherjea M, Sachdev S, Randall JD, Sarkar S. Role of the fetal and alpha/beta exons in the function of fast skeletal troponin T isoforms: correlation with altered Ca2+ regulation associated with development. *J Mol Biol* 2005;352:58-71. 10.1016/j.jmb.2005.06.066

(24) Gallon CE, Tschirgi ML, Chandra M. Differences in myofilament calcium sensitivity in rat psoas fibers reconstituted with troponin T isoforms containing the alpha- and beta-exons. *Arch Biochem Biophys* 2006;456:127-34. 10.1016/j.abb.2006.06.008

(25) Pan BS, Potter JD. Two genetically expressed troponin T fragments representing alpha and beta isoforms exhibit functional differences. *J Biol Chem* 1992;267:23052-6.

(26) Wu QL, Jha PK, Du Y, Leavis PC, Sarkar S. Overproduction and rapid purification of human fast skeletal beta troponin T using Escherichia coli expression vectors: functional differences between the alpha and beta isoforms. *Gene* 1995;155:225-30.

(27) Amarasinghe C, Jin JP. N-Terminal Hypervariable Region of Muscle Type Isoforms of Troponin T Differentially Modulates the Affinity of Tropomyosin-Binding Site 1. *Biochemistry* 2015;54:3822-30. 10.1021/acs.biochem.5b00348

(28) Marden JH, Fescemyer HW, Saastamoinen M, MacFarland SP, Vera JC, Frilander MJ, Hanski I. Weight and nutrition affect pre-mRNA splicing of a muscle gene

associated with performance, energetics and life history. *J Exp Biol* 2008;211:3653-60. 10.1242/jeb.023903

(29) Neumann DA. Kinesiology of the Musculoskeletal System: Foundations for Rehabilitation. 2 ed. Elsevier Health Sciences; 2009. 0323039898. url: https://books.google.com/books?id=FeJOAQAAQBAJ&pg=PA614&lpg=PA614&dq=function+of+gastrocnemius+weight+loading&source=bl&ots=BUJHc5vRNy&sig=vRUbub0d7le-K_idhAaG69zm-pg&hl=en&sa=X&ved=0CE4Q6AEwBmoVChMIhqqTwp6PxgIVj5eICh3d7QCI#v=onepage&q=gastrocnemius%20weight%20loading&f=false

(30) Edgerton VR, Smith JL, Simpson DR. Muscle fibre type populations of human leg muscles. *Histochem J* 1975;7:259-66.

(31) Patel NA, Chalfant CE, Watson JE, Wyatt JR, Dean NM, Eichler DC, Cooper DR. Insulin regulates alternative splicing of protein kinase C beta II through a phosphatidylinositol 3-kinase-dependent pathway involving the nuclear serine/arginine-rich splicing factor, SRp40, in skeletal muscle cells. *J Biol Chem* 2001;276:22648-54. 10.1074/jbc.M101260200

(32) Schilder RJ, Kimball SR, Jefferson LS. Cell-autonomous regulation of fast troponin T pre-mRNA alternative splicing in response to mechanical stretch. *Am J Physiol Cell Physiol* 2012;303:C298-307. 10.1152/ajpcell.00400.2011

(33) Kanadia RN, Johnstone KA, Mankodi A, Lungu C, Thornton CA, Esson D, Timmers AM, Hauswirth WW, Swanson MS. A muscleblind knockout model for myotonic dystrophy. *Science* 2003;302:1978-80. 10.1126/science.1088583

(34) Kanadia RN, Shin J, Yuan Y, Beattie SG, Wheeler TM, Thornton CA, Swanson MS. Reversal of RNA missplicing and myotonia after muscleblind overexpression in a mouse poly(CUG) model for myotonic dystrophy. *Proc Natl Acad Sci U S A* 2006;103:11748-53. 10.1073/pnas.0604970103

(35) Vicente-Crespo M, Pascual M, Fernandez-Costa JM, Garcia-Lopez A, Monferrer L, Miranda ME, Zhou L, Artero RD. Drosophila muscleblind is involved in troponin T alternative splicing and apoptosis. *PLoS One* 2008;3:e1613. 10.1371/journal.pone.0001613

(36) Westerblad H, Bruton JD, Katz A. Skeletal muscle: energy metabolism, fiber types, fatigue and adaptability. *Exp Cell Res* 2010;316:3093-9. 10.1016/j.yexcr.2010.05.019

(37) Bonaldo P, Sandri M. Cellular and molecular mechanisms of muscle atrophy. *Dis Model Mech* 2013;6:25-39. 10.1242/dmm.010389

(38) Ciciliot S, Rossi AC, Dyar KA, Blaauw B, Schiaffino S. Muscle type and fiber type specificity in muscle wasting. *Int J Biochem Cell Biol* 2013;45:2191-9. 10.1016/j.biocel.2013.05.016

(39) Spletter ML, Schnorrer F. Transcriptional regulation and alternative splicing cooperate in muscle fiber-type specification in flies and mammals. *Exp Cell Res* 2014;321:90-8. 10.1016/j.yexcr.2013.10.007

(40) Goldspink G. Age-related loss of muscle mass and strength. *J Aging Res* 2012;2012:158279. 10.1155/2012/158279

(41) Allman BL, Rice CL. An age-related shift in the force-frequency relationship affects quadriceps fatigability in old adults. *J Appl Physiol (1985)* 2004;96:1026-32. 10.1152/japplphysiol.00991.2003

(42) Horner AM, Russ DW, Biknevicius AR. Effects of early-stage aging on locomotor dynamics and hindlimb muscle force production in the rat. *J Exp Biol* 2011;214:3588-95. 10.1242/jeb.055087

(43) Metter EJ, Talbot LA, Schrager M, Conwit R. Skeletal muscle strength as a predictor of all-cause mortality in healthy men. *J Gerontol A Biol Sci Med Sci* 2002;57:B359-65.

(44) Strawbridge WJ, Shema SJ, Balfour JL, Higby HR, Kaplan GA. Antecedents of frailty over three decades in an older cohort. *J Gerontol B Psychol Sci Soc Sci* 1998;53:S9-16.

(45) Miljkovic N, Lim JY, Miljkovic I, Frontera WR. Aging of skeletal muscle fibers. *Ann Rehabil Med* 2015;39:155-62. 10.5535/arm.2015.39.2.155

(46) Kelleher AR, Pereira SL, Jefferson LS, Kimball SR. REDD2 Expression in Rat Skeletal Muscle Correlates with Nutrient-Induced Activation of mTORC1: Responses to Aging, Immobilization, and Remobilization. *Am J Physiol Endocrinol Metab* 2014;308:E122-9. 10.1152/ajpendo.00341.2014

(47) Miller MS, Bedrin NG, Callahan DM, Previs MJ, Jennings ME, Ades PA, Maughan DW, Palmer BM, Toth MJ. Age-related slowing of myosin actin cross-bridge kinetics is sex specific and predicts decrements in whole skeletal muscle performance in humans. *J Appl Physiol (1985)* 2013;115:1004-14. 10.1152/japplphysiol.00563.2013

(48) Mitchell WK, Williams J, Atherton P, Larvin M, Lund J, Narici M. Sarcopenia, dynapenia, and the impact of advancing age on human skeletal muscle size and strength; a quantitative review. *Front Physiol* 2012;3:260. 10.3389/fphys.2012.00260

(49) Moore AZ, Caturegli G, Metter EJ, Makrogiannis S, Resnick SM, Harris TB, Ferrucci L. Difference in muscle quality over the adult life span and biological correlates in the Baltimore Longitudinal Study of Aging. *J Am Geriatr Soc* 2014;62:230-6. 10.1111/jgs.12653

(50) Coble J, Schilder RJ, Berg A, Drummond MJ, Rasmussen BB, Kimball SR. Influence of ageing and essential amino acids on quantitative patterns of troponin T alternative splicing in human skeletal muscle. *Applied Physiology, Nutrition, and Metabolism* 2015. 10.1139/apnm-2014-0568

(51) Sandri M, Barberi L, Bijlsma AY, Blaauw B, Dyar KA, Milan G, Mammucari C, Meskers CG, Pallafacchina G, Paoli A, et al. Signalling pathways regulating muscle mass in ageing skeletal muscle: the role of the IGF1-Akt-mTOR-FoxO pathway. *Biogerontology* 2013;14:303-23. 10.1007/s10522-013-9432-9

(52) Malatesta M, Bertoni-Freddari C, Fattoretti P, Baldelli B, Fakan S, Gazzanelli G. Aging and vitamin E deficiency are responsible for altered RNA pathways. *Ann N Y Acad Sci* 2004;1019:379-82. 10.1196/annals.1297.067

(53) Drummond MJ, Dickinson JM, Fry CS, Walker DK, Gundermann DM, Reidy PT, Timmerman KL, Markofski MM, Paddon-Jones D, Rasmussen BB, et al. Bed rest impairs skeletal muscle amino acid transporter expression, mTORC1 signaling, and protein synthesis in response to essential amino acids in older adults. *Am J Physiol Endocrinol Metab* 2012;302:E1113-22. 10.1152/ajpendo.00603.2011

(54) Giangregorio L, McCartney N. Bone loss and muscle atrophy in spinal cord injury: epidemiology, fracture prediction, and rehabilitation strategies. *J Spinal Cord Med* 2006;29:489-500.

(55) Brooks NE, Myburgh KH. Skeletal muscle wasting with disuse atrophy is multi-dimensional: the response and interaction of myonuclei, satellite cells and signaling pathways. *Front Physiol* 2014;5:99. 10.3389/fphys.2014.00099

(56) Baldwin KM, Haddad F, Pandorf CE, Roy RR, Edgerton VR. Alterations in muscle mass and contractile phenotype in response to unloading models: role of transcriptional/pretranslational mechanisms. *Front Physiol* 2013;4:284. 10.3389/fphys.2013.00284

(57) de Boer MD, Maganaris CN, Seynnes OR, Rennie MJ, Narici MV. Time course of muscular, neural and tendinous adaptations to 23 day unilateral lower-limb suspension in young men. *J Physiol* 2007;583:1079-91. 10.1113/jphysiol.2007.135392

(58) Greenhaff PL. The molecular physiology of human limb immobilization and rehabilitation. *Exerc Sport Sci Rev* 2006;34:159-63. 10.1249/01.jes.0000240017.99877.8a

(59) Stevens L, Bastide B, Kischel P, Pette D, Mounier Y. Time-dependent changes in expression of troponin subunit isoforms in unloaded rat soleus muscle. *Am J Physiol Cell Physiol* 2002;282:C1025-30. 10.1152/ajpcell.00252.2001

(60) Yu ZB, Gao F, Feng HZ, Jin JP. Differential regulation of myofilament protein isoforms underlying the contractility changes in skeletal muscle unloading. *Am J Physiol Cell Physiol* 2007;292:C1192-203. 10.1152/ajpcell.00462.2006

(61) Bodine SC, Stitt TN, Gonzalez M, Kline WO, Stover GL, Bauerlein R, Zlotchenko E, Scrimgeour A, Lawrence JC, Glass DJ, et al. Akt/mTOR pathway is a crucial regulator of skeletal muscle hypertrophy and can prevent muscle atrophy in vivo. *Nat Cell Biol* 2001;3:1014-9. 10.1038/ncb1101-1014

(62) Haddad F, Adams GR. Aging-sensitive cellular and molecular mechanisms associated with skeletal muscle hypertrophy. *J Appl Physiol (1985)* 2006;100:1188-203. 10.1152/japplphysiol.01227.2005

(63) Callahan DM, Miller MS, Sweeny AP, Tourville TW, Slauterbeck JR, Savage PD, Maugan DW, Ades PA, Beynnon BD, Toth MJ. Muscle disuse alters skeletal muscle contractile function at the molecular and cellular levels in older adult humans in a sex-specific manner. *J Physiol* 2014;592:4555-73. 10.1113/jphysiol.2014.279034

(64) Miller MS, Callahan DM, Toth MJ. Skeletal muscle myofilament adaptations to aging, disease, and disuse and their effects on whole muscle performance in older adult humans. *Front Physiol* 2014;5:369. 10.3389/fphys.2014.00369

(65) Dirks ML, Wall BT, Nilwik R, Weerts DHJM, Verdijk LB, van Loon LJC. Skeletal Muscle Disuse Atrophy Is Not Attenuated by Dietary Protein Supplementation in Healthy Older Men. *The Journal of Nutrition* 2014;144:1196-203.

(66) Ogden CL, Carroll MD, Kit BK, Flegal KM. Prevalence of childhood and adult obesity in the United States, 2011-2012. *JAMA* 2014;311:806-14. 10.1001/jama.2014.732

(67) Guh DP, Zhang W, Bansback N, Amarsi Z, Birmingham CL, Anis AH. The incidence of co-morbidities related to obesity and overweight: a systematic review and meta-analysis. *BMC Public Health* 2009;9:88. 10.1186/1471-2458-9-88

(68) Flegal KM, Williamson DF, Pamuk ER, Rosenberg HM. Estimating deaths attributable to obesity in the United States. *Am J Public Health* 2004;94:1486-9.

(69) Maffiuletti NA, Ratel S, Sartorio A, Martin V. The Impact of Obesity on In Vivo Human Skeletal Muscle Function. *Current Obesity Reports* 2013;2:251-60. 10.1007/s13679-013-0066-7

(70) Hilton TN, Tuttle LJ, Bohnert KL, Mueller MJ, Sinacore DR. Excessive adipose tissue infiltration in skeletal muscle in individuals with obesity, diabetes mellitus, and peripheral neuropathy: association with performance and function. *Phys Ther* 2008;88:1336-44. 10.2522/ptj.20080079

(71) Hulens M, Vansant G, Claessens AL, Lysens R, Muls E, Rzewnicki R. Health-related quality of life in physically active and sedentary obese women. *Am J Hum Biol* 2002;14:777-85. 10.1002/ajhb.10095

(72) Hulens M, Vansant G, Lysens R, Claessens AL, Muls E. Exercise capacity in lean versus obese women. *Scand J Med Sci Sports* 2001;11:305-9.

(73) Rauch R, Veilleux LN, Rauch F, Bock D, Welisch E, Filler G, Robinson T, Burrill E, Norozi K. Muscle force and power in obese and overweight children. *J Musculoskelet Neuronal Interact* 2012;12:80-3.

(74) Phillips CM, Kesse-Guyot E, McManus R, Hercberg S, Lairon D, Planells R, Roche HM. High dietary saturated fat intake accentuates obesity risk associated with the fat mass and obesity-associated gene in adults. *J Nutr* 2012;142:824-31. 10.3945/jn.111.153460

(75) Nguyen DM, El-Serag HB. The epidemiology of obesity. *Gastroenterol Clin North Am* 2010;39:1-7. 10.1016/j.gtc.2009.12.014

(76) Buettner R, Schölmerich J, Bollheimer LC. High-fat diets: modeling the metabolic disorders of human obesity in rodents. *Obesity (Silver Spring)* 2007;15:798-808. 10.1038/oby.2007.608

(77) Sishi B, Loos B, Ellis B, Smith W, du Toit EF, Engelbrecht AM. Diet-induced obesity alters signalling pathways and induces atrophy and apoptosis in skeletal muscle in a prediabetic rat model. *Exp Physiol* 2011;96:179-93. 10.1113/expphysiol.2010.054189

(78) Akhmedov D, Berdeaux R. The effects of obesity on skeletal muscle regeneration. *Front Physiol* 2013;4:371. 10.3389/fphys.2013.00371

(79) Corcoran MP, Lamon-Fava S, Fielding RA. Skeletal muscle lipid deposition and insulin resistance: effect of dietary fatty acids and exercise. *Am J Clin Nutr* 2007;85:662-77.

(80) Souto Padron de Figueiredo A, Salmon AB, Bruno F, Jimenez F, Martinez HG, Halade GV, Ahuja SS, Clark RA, DeFronzo RA, Abboud HE, et al. Nox2 mediates skeletal muscle insulin resistance induced by a high fat diet. *J Biol Chem* 2015;290:13427-39. 10.1074/jbc.M114.626077

(81) Tremblay F, Lavigne C, Jacques H, Marette A. Defective insulin-induced GLUT4 translocation in skeletal muscle of high fat-fed rats is associated with alterations in both Akt/protein kinase B and atypical protein kinase C (zeta/lambda) activities. *Diabetes* 2001;50:1901-10.

(82) Lee SR, Khamoui AV, Jo E, Park BS, Zourdos MC, Panton LB, Ormsbee MJ, Kim JS. Effects of chronic high-fat feeding on skeletal muscle mass and function in middle-aged mice. *Aging Clin Exp Res* 2015. 10.1007/s40520-015-0316-5

(83) Denies MS, Johnson J, Maliphol AB, Bruno M, Kim A, Rizvi A, Rustici K, Medler S. Diet-induced obesity alters skeletal muscle fiber types of male but not female mice. *Physiol Rep* 2014;2:e00204. 10.1002/phy2.204

(84) de Wilde J, Mohren R, van den Berg S, Boekschoten M, Dijk KW, de Groot P, Müller M, Mariman E, Smit E. Short-term high fat-feeding results in morphological and metabolic adaptations in the skeletal muscle of C57BL/6J mice. *Physiol Genomics* 2008;32:360-9. 10.1152/physiolgenomics.00219.2007

(85) Thomas MM, Trajcevski KE, Coleman SK, Jiang M, Di Michele J, O'Neill HM, Lally JS, Steinberg GR, Hawke TJ. Early oxidative shifts in mouse skeletal muscle morphology with high-fat diet consumption do not lead to functional improvements. *Physiol Rep* 2014;2. 10.14814/phy2.12149

(86) Shortreed KE, Krause MP, Huang JH, Dhanani D, Moradi J, Ceddia RB, Hawke TJ. Muscle-specific adaptations, impaired oxidative capacity and maintenance of contractile function characterize diet-induced obese mouse skeletal muscle. *PLoS One* 2009;4:e7293. 10.1371/journal.pone.0007293

(87) Ciapaite J, van den Berg SA, Houten SM, Nicolay K, van Dijk KW, Jeneson JA. Fiber-type-specific sensitivities and phenotypic adaptations to dietary fat overload differentially impact fast- versus slow-twitch muscle contractile function in C57BL/6J mice. *J Nutr Biochem* 2015;26:155-64. 10.1016/j.jnutbio.2014.09.014

(88) Jasuja R, LeBrasseur NK. Regenerating skeletal muscle in the face of aging and disease. *Am J Phys Med Rehabil* 2014;93:S88-96. 10.1097/PHM.0000000000000118

(89) Kimball SR, O'Malley JP, Anthony JC, Crozier SJ, Jefferson LS. Assessment of biomarkers of protein anabolism in skeletal muscle during the life span of the rat: sarcopenia despite elevated protein synthesis. *Am J Physiol Endocrinol Metab* 2004;287:E772-80. 10.1152/ajpendo.00535.2003

(90) Goldspink G. Impairment of IGF-I gene splicing and MGF expression associated with muscle wasting. *Int J Biochem Cell Biol* 2006;38:481-9.

(91) Stevenson EJ, Giresi PG, Koncarevic A, Kandarian SC. Global analysis of gene expression patterns during disuse atrophy in rat skeletal muscle. *J Physiol* 2003;551:33-48. 10.1113/jphysiol.2003.044701

(92) Phillips CM, Goumidi L, Bertrais S, Field MR, McManus R, Hercberg S, Lairon D, Planells R, Roche HM. Dietary saturated fat, gender and genetic variation at the TCF7L2 locus predict the development of metabolic syndrome. *J Nutr Biochem* 2012;23:239-44. 10.1016/j.jnutbio.2010.11.020

(93) Lutz TA, Woods SC. Overview of animal models of obesity. *Curr Protoc Pharmacol* 2012;Chapter 5:Unit5.61. 10.1002/0471141755.ph0561s58

(94) Nilsson C, Raun K, Yan FF, Larsen MO, Tang-Christensen M. Laboratory animals as surrogate models of human obesity. *Acta Pharmacol Sin* 2012;33:173-81. 10.1038/aps.2011.203

(95) Duca FA, Sakar Y, Lepage P, Devime F, Langelier B, Doré J, Covasa M. Replication of obesity and associated signaling pathways through transfer of microbiota from obese-prone rats. *Diabetes* 2014;63:1624-36. 10.2337/db13-1526

(96) Levin BE, Dunn-Meynell AA. Defense of body weight against chronic caloric restriction in obesity-prone and -resistant rats. *Am J Physiol Regul Integr Comp Physiol* 2000;278:R231-7.

(97) Lira ME, Loomis AK, Paciga SA, Lloyd DB, Thompson JF. Expression of CETP and of splice variants induces the same level of ER stress despite secretion efficiency differences. *J Lipid Res* 2008;49:1955-62. 10.1194/jlr.M800078-JLR200

(98) Dietary Guidelines for Americans. 2010. url: http://www.health.gov/dietaryguidelines/2010.asp - overview

(99) Willett WC, Leibel RL. Dietary fat is not a major determinant of body fat. *Am J Med* 2002;113 Suppl 9B:47S-59S.

(100) Xu T, Yang L, Yan C, Wang X, Huang P, Zhao F, Zhao L, Zhang M, Jia W, Liu Y. The IRE1α-XBP1 pathway regulates metabolic stress-induced compensatory proliferation of pancreatic β-cells. *Cell Res* 2014;24:1137-40. 10.1038/cr.2014.55

(101) Wang D, Wei Y, Pagliassotti MJ. Saturated fatty acids promote endoplasmic reticulum stress and liver injury in rats with hepatic steatosis. *Endocrinology* 2006;147:943-51. 10.1210/en.2005-0570

(102) Harada N, Yamada Y, Tsukiyama K, Yamada C, Nakamura Y, Mukai E, Hamasaki A, Liu X, Toyoda K, Seino Y, et al. A novel GIP receptor splice variant influences GIP sensitivity of pancreatic beta-cells in obese mice. *Am J Physiol Endocrinol Metab* 2008;294:E61-8. 10.1152/ajpendo.00358.2007

(103) Ahlqvist E, Osmark P, Kuulasmaa T, Pilgaard K, Omar B, Brøns C, Kotova O, Zetterqvist AV, Stancáková A, Jonsson A, et al. Link between GIP and osteopontin in adipose tissue and insulin resistance. *Diabetes* 2013;62:2088-94. 10.2337/db12-0976

(104) Soukup T, Zacharová G, Smerdu V. Fibre type composition of soleus and extensor digitorum longus muscles in normal female inbred Lewis rats. *Acta Histochem* 2002;104:399-405. 10.1078/0065-1281-00660

(105) Patel NA, Kaneko S, Apostolatos HS, Bae SS, Watson JE, Davidowitz K, Chappell DS, Birnbaum MJ, Cheng JQ, Cooper DR. Molecular and genetic studies imply Akt-mediated signaling promotes protein kinase CbetaII alternative splicing via phosphorylation of serine/arginine-rich splicing factor SRp40. *J Biol Chem* 2005;280:14302-9. 10.1074/jbc.M411485200

(106) Pedrotti S, Giudice J, Dagnino-Acosta A, Knoblauch M, Singh RK, Hanna A, Mo Q, Hicks J, Hamilton S, Cooper TA. The RNA-binding protein Rbfox1 regulates splicing required for skeletal muscle structure and function. *Hum Mol Genet* 2015;24:2360-74. 10.1093/hmg/ddv003

(107) Cohen S, Nathan JA, Goldberg AL. Muscle wasting in disease: molecular mechanisms and promising therapies. *Nat Rev Drug Discov* 2015;14:58-74. 10.1038/nrd4467